

ORIGINAL ARTICLE

Photosynthetic responses to temperature across the tropics: a meta-analytic approach

Kelsey R. Carter^{1,2,*}, Molly A. Cavalieri², Owen K. Atkin³, Nur H. A. Bahar³, Alexander W. Cheesman⁴, Zineb Choury⁵, Kristine Y. Crous⁵, Christopher E. Doughty⁶, Mirindi E. Dusenge^{3,7}, Kim S. Ely^{8,9}, John R. Evans³, Jéssica Fonseca da Silva^{10,11,12}, Alida C. Mau², Belinda E. Medlyn⁵, Patrick Meir¹³, Richard J. Norby^{1,14}, Jennifer Read¹⁵, Sasha C. Reed¹⁶, Peter B. Reich^{5,17,18}, Alistair Rogers^{8,9}, Shawn P Serbin¹⁹, Martijn Slot²⁰, Elsa C. Schwartz², Edgard S. Tribuzy²¹, Johan Uddling²², Angelica Vårhammar⁵, Anthony P. Walker¹, Klaus Winter²⁰, Tana E. Wood¹⁰ and Jin Wu²³

¹Environmental Sciences Division and Climate Change Science Institute, Oak Ridge National Laboratory, Oak Ridge, TN, USA,

²College of Forest Resources and Environmental Science, Michigan Technological University, Houghton, MI, USA, ³Division of Plant Sciences, Research School of Biology, The Australian National University, Canberra, ACT 2601, Australia, ⁴James Cook University, College of Science and Engineering, Cairns, QLD, 4878, Australia, ⁵Hawkesbury Institute for the Environment, Western Sydney University, Penrith, NSW 2751, Australia, ⁶School of Informatics, Computing, and Cyber Systems, Northern Arizona University, Flagstaff, AZ, USA, ⁷Department of Biology, Mount Allison University, Sackville, New Brunswick, E4L 1E4, Canada, ⁸Environmental and Climate Sciences Department, Brookhaven National Laboratory, Upton, NY, USA, ⁹Climate and Ecosystem Sciences Division, Lawrence Berkeley National Laboratory, Berkeley, CA 94720, USA, ¹⁰U.S. Department of Agriculture, Forest Service, International Institute of Tropical Forestry, Río Piedras, PR, USA, ¹¹Center for Applied Tropical Ecology and Conservation, University of Puerto Rico, Río Piedras, PR, USA, ¹²Department of Biology, University of Puerto Rico, Río Piedras, PR, USA, ¹³School of Geosciences, University of Edinburgh, Edinburgh, UK, ¹⁴Department of Ecology and Evolutionary Biology, University of Tennessee, Knoxville, TN, USA, ¹⁵School of Biological Sciences, Monash University, Victoria 3800, Australia, ¹⁶U.S. Geological Survey, Southwest Biological Science Center, Moab, UT, USA, ¹⁷Institute for Global Change Biology, and School for the Environment and Sustainability, University of Michigan, Ann Arbor, MI 48109, USA, ¹⁸Department of Forest Resources, University of Minnesota, St. Paul, MN, USA, ¹⁹Biospheric Sciences Laboratory, NASA Goddard Space Flight Center, Greenbelt, MD, USA, ²⁰Smithsonian Tropical Research Institute, Apartado Postal 0843-03092, Panama, Republic of Panama, ²¹Instituto de Biodiversidade e Florestas, Universidade Federal do Oeste do Pará (UFOPA), CEP 68035-110, Santarém, PA, Brazil, ²²Department of Biological and Environmental Sciences, University of Gothenburg, Gothenburg, Sweden, and ²³School of Biological Sciences, University of Hong Kong, Pokfulam, Hong Kong

*For correspondence. E-mail carterkr@ornl.gov

Received: 26 July 2024 Returned for revision: 3 November 2024 Editorial decision: 25 November 2024 Accepted: 10 December 2024

• **Background and Aims** Tropical forests exchange more carbon dioxide (CO₂) with the atmosphere than any other terrestrial biome. Yet, uncertainty in the projected carbon balance over the next century is roughly three times greater for the tropics than other for ecosystems. Our limited knowledge of tropical plant physiological responses, including photosynthetic, to climate change is a substantial source of uncertainty in our ability to forecast the global terrestrial carbon sink.

• **Methods** We used a meta-analytic approach, focusing on tropical photosynthetic temperature responses, to address this knowledge gap. Our dataset, gleaned from 18 independent studies, included leaf-level light-saturated photosynthetic (A_{sat}) temperature responses from 108 woody species, with additional temperature parameters (35 species) and rates (250 species) of both maximum rates of electron transport (J_{max}) and Rubisco carboxylation (V_{cmax}). We investigated how these parameters responded to mean annual temperature (MAT), temperature variability, aridity and elevation, as well as also how responses differed among successional strategy, leaf habit and light environment.

• **Key Results** Optimum temperatures for A_{sat} (T_{optA}) and J_{max} (T_{optJ}) increased with MAT but not for V_{cmax} (T_{optV}). Although photosynthetic rates were higher for 'light' than 'shaded' leaves, light conditions did not generate differences in temperature response parameters. T_{optA} did not differ with successional strategy, but early successional species had ~4 °C wider thermal niches than mid/late species. Semi-deciduous species had ~1 °C higher T_{optA}

than broadleaf evergreen species. Most global modelling efforts consider all tropical forests as a single ‘broadleaf evergreen’ functional type, but our data show that tropical species with different leaf habits display distinct temperature responses that should be included in modelling efforts.

- **Conclusions** This novel research will inform modelling efforts to quantify tropical ecosystem carbon cycling and provide more accurate representations of how these key ecosystems will respond to altered temperature patterns in the face of climate warming.

Key words: $A-C_i$ curves, maximum rate of photosynthetic electron transport (J_{\max}), maximum rate of Rubisco carboxylation (V_{\max}), meta-analysis, photosynthesis, temperature response, tropics.

INTRODUCTION

Tropical forests have been characterized as one of the biomes with the greatest uncertainty regarding the accuracy of large-scale models in estimating carbon fluxes (Booth *et al.*, 2012; Cavalieri *et al.*, 2015; Lombardozzi *et al.*, 2015; Mercado *et al.*, 2018). Addressing this information gap is critical because tropical forests have high biomass and cycle large amounts of carbon (Dixon *et al.*, 1994; Pan *et al.*, 2013; Tagesson *et al.*, 2020), and thus alterations in tropical forest carbon uptake would probably significantly affect global carbon cycling (Anderegg *et al.*, 2015). In addition, these forests are projected to surpass their historical climate margin, entering into novel climate conditions within the next quarter century (Williams *et al.*, 2007; but see Jaramillo *et al.*, 2010), a trend anticipated to occur sooner for the tropics than other global regions (Diffenbaugh and Scherer, 2011; Mora *et al.*, 2013; Doughty *et al.*, 2023). Some tropical forests are already believed to be operating near or beyond their photosynthetic thermal optima (Doughty and Goulden, 2008; Vårhammar *et al.*, 2015; Mau *et al.*, 2018; Dusenge *et al.*, 2021; Doughty *et al.*, 2023), making them particularly vulnerable to the effects of climate warming on carbon uptake.

Due to the significant uncertainties around how the tropical forest biome will respond to continued global change, better representation of vegetation processes is needed to more accurately inform Earth system and dynamic vegetation models (Friedlingstein *et al.*, 2006; Matthews *et al.*, 2007; Booth *et al.*, 2012; Rogers *et al.*, 2017; Fisher *et al.*, 2018). In particular, quantifying photosynthetic temperature responses of tropical species will help to reduce model uncertainty (Matthews *et al.*, 2007; Booth *et al.*, 2012). Photosynthesis has a peaked response to temperature, where the rate of photosynthesis increases and then declines after the optimum temperature (T_{optA} ; Table 1) is reached. The components of photosynthetic decline beyond the thermal optimum can be examined by exploring stomatal conductance and the underlying biochemical processes that control photosynthesis. These biochemical processes include the maximum rate of carbon dioxide (CO_2) fixation by Rubisco (V_{\max}) and the maximum rate of photosynthetic electron transport (J_{\max}), both of which are derived by a well-established biochemical model (Farquhar *et al.*, 1980; von Caemmerer and Farquhar, 1981). Global vegetation models use the temperature response parameters of these biochemical processes controlling photosynthesis to predict carbon uptake at wider scales (Kattge *et al.*, 2009; Lin *et al.*, 2012; Smith and Dukes, 2013; Mercado *et al.*, 2018; Oliver *et al.*, 2022).

Considerable efforts have been made to quantify these photosynthetic response parameters at the global scale (Medlyn *et al.*, 2002; Kattge and Knorr, 2007; Yamori *et al.*, 2014;

Kumarathunge *et al.*, 2019; Crous *et al.*, 2022). These studies show that species can (but may not) acclimate to their growth environment, and algorithms developed in Kattge and Knorr (2007) have been implemented in some Earth system and vegetation models for more accurate representation of photosynthetic acclimation (e.g. Arneth *et al.*, 2012; Lombardozzi *et al.*, 2015; Smith *et al.*, 2016; Mercado *et al.*, 2018). However, Kattge and Knorr (2007) did not have enough data to represent tropical species in their meta-analysis. As a result, carbon models are probably biased in projecting tropical biome temperature responses. More recently, Kumarathunge *et al.* (2019) published updated algorithms including six datasets from tropical forests which will undoubtedly improve global carbon models (Zarakas *et al.*, 2024). Even so, because tropical forests cycle a disproportionate amount of carbon, specific investigations of tropical photosynthetic responses to temperature based on plant function and growth strategy will further minimize uncertainty for this crucial biome (Booth *et al.*, 2012).

There is strong evidence suggesting that, across the globe, T_{opt} is determined by the plant’s current growth temperature (Berry and Björkman, 1980; Kattge and Knorr, 2007; Kumarathunge *et al.*, 2019). Genetic variation also plays an important role in determining species’ ability to acclimate and adjust to their growth temperatures (Berry and Björkman, 1980; Yamori *et al.*, 2014; Crous *et al.*, 2022; but see Kumarathunge *et al.*, 2019). However, it is still unclear whether this holds true within tropical ecosystems. Studies of photosynthetic temperature responses of tropical forest species provide evidence that T_{opt} is either closely associated with mean (Kositsup *et al.*, 2009; Vargas and Cordero, 2013; Tan *et al.*, 2017) or maximum air temperature (Read, 1990; Slot and Winter, 2017a; Mau *et al.*, 2018). Historically, these forests have been thought to have little capacity to acclimate to temperature changes because they have evolved under low variability in diurnal, seasonal and inter-annual ambient air temperature (Janzen, 1967; Read, 1990; Battaglia *et al.*, 1996; Cunningham and Read, 2002). More recent studies have found evidence that tropical leaves are capable of acclimation to the temperature where they are grown (Scafaro *et al.*, 2017; Slot and Winter, 2017b; Choury *et al.*, 2022; Wittemann *et al.*, 2022; Cox *et al.*, 2023), but not for all species (Cunningham and Read, 2003; Slot *et al.*, 2014; Vårhammar *et al.*, 2015; Carter *et al.*, 2020, 2021; Dusenge *et al.*, 2021; Crous *et al.*, 2022; Kullberg *et al.*, 2023) and successional strategy probably influences the response (Mujawamariya *et al.*, 2023). The few studies investigating J_{\max} optimum temperature (T_{optJ}) and V_{\max} optimum temperature (T_{optV}) on tropical species suggest that both traits are closely associated with their home climate and most species are unable to adjust to higher growth temperatures (Slot and Winter, 2017b; Dusenge *et al.*, 2021; but see Wittemann *et al.*, 2022).

TABLE I. Abbreviations and descriptions

Variable	Description	Units
AC_i	Net photosynthetic assimilation at a range of leaf internal CO_2 concentrations	Unitless
AI	Aridity index, calculated as the mean annual precipitation divided by the mean annual evapotranspiration	Unitless
A_{sat}	Light-saturated photosynthesis, estimated from light response curves	$\mu\text{mol m}^{-2} \text{s}^{-1}$
A_{opt}	The value of A_{sat} at the optimum temperature	$\mu\text{mol m}^{-2} \text{s}^{-1}$
A_{25}	Rate of A_{sat} at 25 °C	$\mu\text{mol m}^{-2} \text{s}^{-1}$
E_{av}	The activation energy of the V_{cmax} temperature response curve	kJ mol^{-1}
E_{aj}	The activation energy of the J_{max} temperature response curve	kJ mol^{-1}
g_s	Stomatal conductance	$\text{mol m}^{-2} \text{s}^{-1}$
J_{max}	The maximum rate of photosynthetic electron transport	$\mu\text{mol m}^{-2} \text{s}^{-1}$
J_{25}	The rate of J_{max} at 25 °C	$\mu\text{mol m}^{-2} \text{s}^{-1}$
$J:V$	The ratio between J_{25} and V_{25}	Unitless
k_{opt}	The value of J_{max} or V_{cmax} at the optimum temperature	$\mu\text{mol m}^{-2} \text{s}^{-1}$
MAT	Mean annual temperature	°C
T_{leaf}	Leaf temperature	°C
T_{optA}	The optimum temperature for A_{sat}	°C
T_{optJ}	Optimum temperature of photosynthetic electron transport	°C
T_{optV}	Optimum temperature for Rubisco carboxylation	°C
T_{range}	Mean annual temperature range	°C
V_{cmax}	Maximum rate of Rubisco carboxylation	$\mu\text{mol m}^{-2} \text{s}^{-1}$
VPD	Vapour pressure deficit	kPa
V_{25}	The rate of V_{cmax} at 25 °C	$\mu\text{mol m}^{-2} \text{s}^{-1}$
Ω	The difference in T_{opt} and the temperature where the rate of photosynthesis is 37 % of T_{opt}	°C

Additionally, a common garden study by Vårhammar *et al.* (2015) found that tropical species that originate from areas with lower temperatures have lower optimum temperatures for J_{max} than species that originate from warmer areas. This variation of photosynthetic temperature responses in tropical forests suggests that, in order to accurately model global carbon fluxes, we need to better understand the drivers of temperature responses for critical photosynthetic parameters in tropical systems.

Growth conditions and ecological successions can also affect plant photosynthetic responses to temperature (Yamori *et al.*, 2014; Dusenge *et al.*, 2019), and these differences are rarely incorporated into vegetation models (Lombardozzi *et al.*, 2015; Smith *et al.*, 2016; Mercado *et al.*, 2018). Growth strategies are often characterized by their successional strategy, with some forms, such as early successional species and lianas, incorporating fast growth as juveniles, while late successional and evergreen species employ slower growth as juveniles (Bloom *et al.*, 1985; Box, 1996; Wright *et al.*, 2004; Michaletz *et al.*, 2016). Due to higher radiation reaching deeper into the canopy, early successional forests have more variable land surface temperature fluxes than late successional forests (Cao and Sanchez-Azofeifa, 2017), suggesting that seedlings adapted to this environment may have a greater plasticity to adjust T_{opt} to their fluctuating growth environment. Studies of canopy species in Panama found that early successional seedlings had a higher T_{opt} than late successional seedlings (Slot *et al.*, 2016; Slot and Winter, 2018). However, those results were not replicated for

mature canopy trees (Slot and Winter, 2017a), suggesting that successional type T_{opt} differences are driven primarily by trees at the immature seedling and sapling stages.

Tropical trees with differing leaf habits (i.e. evergreen vs. deciduous) may also employ different temperature responses. For example, species with shorter-lived leaves have a greater variability in leaf phenotypes, making them more responsive to seasonal changes (Kitajima *et al.*, 1997). Compared to longer-lived evergreen leaves, shorter-lived deciduous leaves are hypothesized to have broader photosynthetic temperature response curves (i.e. thermal niches; Michaletz *et al.*, 2016). Broad- and needleleaf evergreen species have been found to be less able to increase their growth rates in higher temperatures than deciduous species (Way and Oren, 2010; Way and Yamori, 2014; Yamori *et al.*, 2014; Reich *et al.*, 2022). Recently, Crous *et al.* (2022) found that needleleaf evergreen species' photosynthetic and respiration rates declined more with warming compared to broadleaf evergreen species. This, in addition to longer-lived leaves having lower photosynthetic capacity (Niinemets, 2007), and lower rates of photosynthesis (Wright *et al.*, 2004), suggests that evergreen and deciduous species may have different capabilities to respond to their growth environment.

Light availability may also play a role in modulating plant photosynthetic responses to temperature (Niinemets, 2007). Models of canopy photosynthesis and global primary productivity often separate leaves into 'sun' and 'shade' leaves, as they have different photosynthetic responses to irradiance (Sinclair

et al., 1976; De Pury and Farquhar, 1997; Wang and Leuning, 1998; Ryu *et al.*, 2011). Because leaf temperature is strongly influenced by irradiance (Rey-Sánchez *et al.*, 2016; Fauset *et al.*, 2018; Miller *et al.*, 2021; Crous *et al.*, 2023), it should follow that sun leaves that have developed under higher irradiance are acclimated to operate at higher temperatures. However, comparisons of leaves growing in different light environments in tropical forests have found large differences in photosynthetic capacity but little to no differences in photosynthetic temperature response (Pearcy, 1987; Hernández *et al.*, 2020), or thermotolerance (Slot *et al.*, 2019), between sun and shade leaves. The limited evidence that we have comparing tropical temperature responses of sun and shade leaves suggests that light may play a large role in determining overall carbon gain but only a minor role for leaves' photosynthetic temperature responses.

Rainfall and moisture regimes also play a role in controlling plant photosynthesis, which can lead to restrictions on temperature response parameters. In general, drier conditions can induce stomatal closure, slowing the rate of photosynthesis and decreasing tropical forest productivity (Cavaleri *et al.*, 2017; Santos *et al.*, 2018; Van Schaik *et al.*, 2018; Kumarathunge *et al.*, 2020; Mujawamariya *et al.*, 2023). However, drier conditions are also associated with less rainfall and cloud cover, and a higher light environment can directly increase ecosystem productivity (Carswell *et al.*, 2002). Ecosystem-scale studies show gross primary productivity (GPP) can either increase in the dry season (Goulden *et al.*, 2004; Yan *et al.*, 2013; Wu *et al.*, 2016; Green *et al.*, 2020) or remain constant between seasons (Carswell *et al.*, 2002; Yan *et al.*, 2013; Guan *et al.*, 2015), suggesting that tropical forests can sustain higher GPP during the higher dry-season atmospheric water stress if they are not stomatal conductance-limited. Across two Panamanian tropical systems, a leaf-level study showed that, when compared to a wet forest, seasonally dry forests can have higher rates of photosynthesis and higher optimum temperatures that correspond to their higher growth temperatures (Slot and Winter, 2017a). Within a Puerto Rican tropical forest, drier soil was associated with higher optimum temperatures but lower rates of photosynthesis (Carter *et al.*, 2020). These studies suggest that optimum temperatures could be positively correlated with drier tropical systems.

To better understand tropical net photosynthetic and biochemical responses to temperature, we used a meta-analytic approach to quantify how photosynthetic temperature response parameters respond to different climate and growth environment factors using already established temperature response functions (Medlyn *et al.*, 2002; June *et al.*, 2004). We hypothesize that (1) light-saturated photosynthetic optimum temperatures (T_{optA}) will be positively correlated with mean annual temperature (MAT) due to positive shifts in V_{cmax} temperature response parameters. We similarly hypothesize that, due to indirect environmental effects of higher light availability, (2) temperature optima will decrease with rising aridity index (AI) (decrease in wetter ecosystems). We also compare temperature response variables of leaves grown in different light environments (sun vs. shade), growth environments (*in situ* vs. *ex situ* or field vs. chamber/glasshouse), leaf habits (evergreen vs. drought semi-deciduous) and successional strategy (early vs. mid-late). We predicted that (3) sun leaves would have higher photosynthetic rates than shade leaves; but that T_{opt} would not differ between

different light environments. Additionally, we predicted that (4) T_{opt} of early successional species will not differ from that of late successional species and (5) broadleaf evergreen leaves would have a narrower thermal niche and lower T_{opt} than semi-deciduous species. Lastly, we aimed to estimate the most important individual environmental drivers to best predict the temperature parameters of both net photosynthesis and the biochemical reactions driving photosynthesis.

METHODS

Meta-analysis data collection and selection

For this meta-analysis, we gathered datasets where photosynthetic measurements were collected at different leaf temperatures on woody (trees, shrubs and lianas) tropical species. These data come in the form of net photosynthesis measured at saturating light conditions (A_{sat}) vs. leaf temperature (T_{leaf}) response curves, A_{sat} vs. T_{leaf} estimated from photosynthetic light response curves at different temperatures, biochemical parameters (V_{cmax} and J_{max}) vs. T_{leaf} response curves (estimated from net assimilation response to different leaf internal CO_2 concentrations, $A-C_i$ curves, measured at different temperatures), and measurements of A_{sat} and $A-C_i$ curves at multiple ambient temperatures through time. Data were gathered from woody species in forested systems within the tropical latitudes ($23^{\circ}26'10.6''\text{N}$, $23^{\circ}26'10.6''\text{S}$), including tropical montane systems. We obtained our data by approaching research groups for unpublished data and searching 'photosynthesis' 'tropical' 'temperature' on Web of Science (Supplementary Data Fig. S1). This resulted in 18 datasets with representation in Africa (2), Oceania (6), North America (8) and South America (3). No studies were identified from the Asian continent. Site-specific climate data from the years 1970–2000 were collected from the WorldClim database (Fick and Hijmans, 2017) using provided latitude and longitudinal data. Latitude and longitude were designated as the location where plants grew, except for data from Read (1990), which were obtained with plants that were grown in a chamber. In this specific case, seeding source location was used for latitude and longitude and MAT was designated as the growth chamber temperature. Data were extracted from the WorldClim database using the 'getData' function in the 'raster' package in R v.3.5.0 (R Core Team, 2020). AI was calculated as mean annual precipitation divided by mean annual potential evapotranspiration (Greve and Seneviratne, 2015), where both variables were collected from WorldClim. Higher AI indicates a less arid system. AI was only used from *in situ* datasets, i.e. we excluded glasshouse, growth chamber and arboretum grown individuals from this analysis. Successional stage and leaf habit (raingreen semi-deciduous or evergreen; Poulter *et al.*, 2015) were either provided by the contributing data author or extracted from the literature. Species that were classified as 'pioneer' and 'shade-intolerant' were designated as 'early successional'. If the species was classified as 'shade-tolerant' it was considered 'mid/late successional'. When light environment information was available, we used author designations or classified ourselves; where growth chamber, glasshouse, 'open' or 'upper' canopy was considered 'sun' and 'understorey' was considered shade. All samples grown in growth chambers, glasshouses, or transplant studies in arboretums were considered 'ex situ'. All

other growth environments (i.e. ‘field collected’) were designated as ‘*in situ*’. We gathered photosynthetic data in two ways: (1) raw data in the form of photosynthetic response curves or (2) extraction from published articles. Data were digitized from published articles using Digitize It 2016 v.4.2.0 software (Alcasa). Raw data were provided from both published and unpublished sources. Some of the datasets that were shared with us also included a ‘warming’ treatment. For these data, we only used leaves grown in the ‘control’ environment.

Net photosynthesis parameter extraction

Within individual datasets, means of different species and canopy class (shaded or sun) from the same study were treated as separate, independent samples (Curtis and Wang, 1998).

The net photosynthetic temperature optimum of each sample was extracted from a peaked curve (June et al., 2004):

$$A_{\text{sat}} = A_{\text{opt}} \times e^{-\left(\frac{T_{\text{leaf}} - T_{\text{optA}}}{\Omega}\right)^2} \quad (1)$$

where A_{sat} ($\mu\text{mol m}^{-2} \text{s}^{-1}$) is the rate of net assimilation at the leaf temperature (T_{leaf}) in $^{\circ}\text{C}$, T_{optA} ($^{\circ}\text{C}$) is the optimum temperature for photosynthesis, and A_{opt} ($\mu\text{mol m}^{-2} \text{s}^{-1}$) is the rate of photosynthesis at T_{optA} . Ω , or net photosynthetic thermal niche, is the temperature difference from T_{optA} where photosynthesis declines to 37 % of A_{opt} . Ω ($^{\circ}\text{C}$) describes the width of the response curve peak, where wide curves have a higher Ω and narrower curves have a lower Ω . Prior to fitting eqn (1), A_{sat} from each dataset was individually inspected for outliers. Outliers were removed only when they were clearly erroneous, such as $A_{\text{sat}} < 0 \mu\text{mol m}^{-2} \text{s}^{-1}$ that were not clearly caused by high temperatures. In addition, data points with $C_i < 0$ were removed as they were considered bad measurements. In total, we removed 402 data points, 2.79 % of our A_{sat} data.

To compare the rates of net photosynthesis across studies, we extracted the rate at 25°C (A_{25}) by allowing T_{leaf} to equal 25 in eqn (1) for each set of extracted temperature parameters. This standard temperature was selected because it is similar to the average MAT (25.5°C) in our dataset and is often used as a standard so photosynthetic rates are widely comparable across studies. Using similar methods as Kumarathunge et al. (2019), we further increased the size of our dataset by extracting A_{sat} values from photosynthetic response to internal CO_2 concentration ($A-C_i$) curves. For these data, we extracted the first data point taken at ambient CO_2 concentrations and saturating irradiance. Values of A_{sat} were kept only if the C_i values were between 275 and 410 ppm. Forty additional curves were added to the A_{sat} dataset using this method. One dataset measured light response curves at different temperatures. A_{sat} was estimated by extracting the light-saturated photosynthetic rate from light response curves using a non-rectangular curve (Marshall and Biscoe, 1980), and fitting A_{sat} to eqn (1). A total of 111 A_{sat} temperature response curve samples were successfully fitted using eqn (1).

Biochemical parameter extraction

Biochemical rates, J_{max} and V_{cmax} , were estimated from $A-C_i$ curves. Most datasets collected $A-C_i$ curves starting at an ambient CO_2 concentration, 360–410 ppm. $A-C_i$ curves were

obtained by gradually decreasing the CO_2 below ambient concentrations (to as low as 0 ppm). CO_2 concentrations were then brought back up to ambient levels and then gradually increased to saturating concentrations (up to 2100 ppm). Prior to fitting the $A-C_i$ curves, data points outside $0 < C_i < 2200$ ppm were removed from the dataset as they were beyond the range of CO_2 concentration given to the leaf. We further removed datapoints where A_{sat} was smaller than -10 and greater than $70 \mu\text{mol m}^{-2} \text{s}^{-1}$ as they were not considered reasonable A_{sat} rates. In total we removed less than 0.5 % of total $A-C_i$ datapoints. J_{max} and V_{cmax} were obtained using the default fit method with ‘Tcorrect = FALSE’ in the ‘fitaci’ function from the ‘plantecophys’ package (Duursma, 2015) in R v.3.5.0 (R Core Team, 2020), which extracts parameters using the Farquhar, von Caemmerer and Berry model (FvCB model; Farquhar et al., 1980; von Caemmerer and Farquhar, 1981). We further looked at the fitted $A-C_i$ curves and individually removed curves with poor fits. We further removed curves where fitted J_{max} and V_{cmax} values were less than $0 \mu\text{mol m}^{-2} \text{s}^{-1}$, as this is not possible for correctly fit curves. After the initial data exclusion, we removed outliers where J_{max} or V_{cmax} were clearly erroneous by looking at qq plots and histograms of each dataset. In total, 7.8 % or 102 $A-C_i$ curves were removed from the initial dataset.

Biochemical temperature response parameters for J_{max} and V_{cmax} were extracted using the peaked Arrhenius function (Medlyn et al., 2002):

$$(T_k) = (k_{\text{opt}}) \frac{H_d \exp\left(\frac{E_a(T_k - T_{\text{opt}})}{(T_k R T_{\text{opt}})}\right)}{H_d - E_a \left[1 - \exp\left(\frac{H_d(T_k - T_{\text{opt}})}{(T_k R T_{\text{opt}})}\right)\right]} \quad (2)$$

where T_k is the measured leaf temperature in Kelvin, (k_{opt}) is the value of J_{max} or V_{cmax} at the optimum temperature ($\mu\text{mol m}^{-2} \text{s}^{-1}$), E_a is the activation energy in the Arrhenius function (kJ mol^{-1}), or exponential increase in J_{max} or V_{cmax} before T_{opt} , H_d is the deactivation energy of J_{max} or V_{cmax} after T_{opt} (kJ mol^{-1}) and R is the universal gas constant ($8.314 \text{ J K}^{-1} \text{ mol}^{-1}$). To avoid over-parameterization of the temperature response function, we set $H_d = 200 \text{ kJ mol}^{-1}$ and estimated T_{opt} , k_{opt} and E_a from eqn (2). Each individual curve was examined and curves were removed if T_{opt} , k_{opt} or E_a values were over or underestimated, e.g. visually estimated T_{opt} was clearly higher or lower than model estimations which was often due to too few temperatures used to produce the curve, resulting in $35 V_{\text{cmax}}$ and $35 J_{\text{max}}$ temperature response curves.

We extracted the rate of V_{cmax} (V_{25}) and J_{max} (J_{25}) at 25°C from $A-C_i$ curves measured from temperatures ranging from 20 to 30°C by setting Tcorrect = ‘TRUE’ in the ‘fitaci’ function. The ratio between J_{25} and V_{25} ($J:V$) was calculated by dividing J_{25} by V_{25} for each individual sample. This resulted in 295 samples in our V_{25} and J_{25} datasets. Version 1.4 of the ‘plantecophys’ package defaults to using temperature fitting parameters estimated from a global analysis of photosynthetic temperature responses that estimated values using (Medlyn et al., 2002):

$$T_k = k_{25} \exp\left[\frac{E_a(T_k - 298)}{(298 R T_k)}\right] \frac{1 + \exp\left(\frac{298 S - H_d}{298 R}\right)}{1 + \exp\left(\frac{T_k S - H_d}{T_k R}\right)} \quad (3)$$

where ΔS is an entropy term. We estimated J_{25} and V_{25} using the default ‘global’ parameters and this study’s tropical estimations of E_a and ΔS (Supplementary Data Table S3) and made comparisons of the two fitting estimations.

Meta-analytic statistical analyses

Biases for sample size were accounted for by weighting each extracted parameter with the number of observations that were used in each temperature response curve. The weighting factor was calculated as (Hedges and Olkin, 1985; Gurevitch *et al.*, 1992):

$$J = 1 - \left(\frac{3}{4(n-1)} \right) \quad (4)$$

where J is the weighting factor and n is the number of data points used to fit each temperature response curve (Supplementary Data Fig. S2). The weighted mean was incorporated into the linear model by adding J into the ‘weights’ weighting factor component of the ‘lmer’ function in the ‘lme4’ package in R (Bates *et al.*, 2015). All data analyses were performed in R v.3.5.0 (R Core Team, 2020).

Mixed effects models were used to compare global and tropical V_{cmax} and J_{max} activation energies (E_{av} and E_{aj} , respectively) and entropy terms (ΔS_v and ΔS_j , respectively), where data source was used as the random intercept. Mixed effects models were also used to investigate relationships between A_{sat} and biochemical parameters (T_{opt} , T_{optA} , T_{optV} , A_{25} , V_{25} , J_{25} , Ω , E_{av} and E_{aj}) and individual climate variables. We found high collinearity between MAT and elevation (Supplementary Data Fig. S3); therefore, elevation was removed from the individual bivariate regression models. We removed elevation as a continuous variable and grouped the data into four elevational groups (0–500, 501–1000, 1001–2000 and >2000 m) to visually show the role that elevation played in our climate range for all bivariate regressions. Mixed effect models were also used to compare leaf habit, successional type and growth conditions, using $\alpha < 0.05$. Due to available characterizations for our dataset, light environment (sun or shade) and leaf habit (deciduous or evergreen) were compared only for A_{sat} parameters. Successional type (early or late) and growth environment (*in* or *ex situ*) were compared for both A_{sat} and biochemical parameters (summary of samples used in each categorical analysis included in Table S2). Estimated J_{25} and V_{25} were compared between the default ‘plantecophys’ package and our parameter estimates using a mixed effects model as described above.

High variance inflation factors (VIFs), a means of identifying potential collinearity, were assessed when we included both MAT and elevation in the same multivariate model, where full models that included all four climate variables (MAT, AI, T_{range} , elevation) had at least one variable with $VIF > 2$ (VIF range 2.02–648.53). VIF on the full model was calculated using the ‘vif’ function in base R. Therefore, we used hierarchical partitioning to quantify which climate variable had the highest explanatory power on parameter (T_{opt} , T_{optA} , T_{optV} , A_{25} , V_{25} , J_{25} , Ω , E_{av} and E_{aj}) variance using the ‘rdacca.hp’ package in R (Lai *et al.*, 2022). Hierarchical partitioning is used in instances of high VIF because it estimates individual importance of predictors in all model subsets, where the subsets also include the

full model (Lai *et al.*, 2022). The individual effects were estimated via hierarchical partitioning and were calculated from the sum of the calculated unique and shared contribution to the overall model’s adjusted R^2 , where the model includes all individual variables of interest. The individual effect can be negative if the unique or shared contribution is negative due to high multicollinearity. In this calculation, the individual effects were added to equal the total adjusted R^2 .

RESULTS

Comparisons of biochemical estimations from global and tropical parameters

Global estimates of biochemical activation energies and entropy terms yielded higher biochemical parameter rates compared to estimates derived from tropical data, suggesting that studies in tropical systems would overestimate V_{25} and J_{25} if using global values. V_{25} and J_{25} estimated from global datasets were both ~7 % higher than those from tropical parameters (Supplementary Data Table S3; Fig. S4A, B), resulting in no discernible difference in JV between parameter estimates (Fig. S4C).

Primary climate variable influences on temperature parameters

In bivariate regressions, the net photosynthetic and electron transport optimum temperature increased with increasing temperature, while the maximum Rubisco carboxylation optimum temperature did not. T_{optA} was positively related to MAT, with MAT alone explaining 37 % of T_{optA} variance (Fig. 1A; Table 2). T_{optA} did not strongly respond to AI or T_{range} (Fig. 2B; Supplementary Data Fig. S5A). T_{optV} did not respond to any of the three climate variables (Figs 1C, D and S5B; Table 2). T_{optJ} increased with rising MAT, which explained 14 % of the variation, and T_{optJ} did not respond to AI or T_{range} (Figs 1E, F and S5C).

While net photosynthetic rate did not show clear relationships with climate variables, the rates of photosynthetic biochemical reactions decreased with a warmer climate. A_{25} did not respond to MAT, AI or T_{range} (Fig. 2A, B; Supplementary Data Fig. S6A; Table 2). V_{25} decreased as MAT rose (marginal $R^2 = 0.20$; Fig. 2C), did not respond to AI (Fig. 2D) and decreased with wider T_{range} (marginal $R^2 = 0.18$; Fig. S6B). Similarly, J_{25} decreased as MAT increased (marginal $R^2 = 0.41$; Fig. 2E), did not respond to AI (Fig. 2F) and increased as T_{range} increased (marginal $R^2 = 0.28$; Fig. S6C). The ratio between J_{max} and V_{cmax} at 25 °C (JV) decreased with rising MAT (marginal $R^2 = 0.28$; Fig. 3A), did not respond to AI (Fig. 3B; Table 2) and increased slightly with a wider T_{range} (marginal $R^2 = 0.06$; Fig. 3C). Neither net photosynthetic thermal niche (Ω) nor the activation energy for V_{cmax} and J_{max} responded to any climate variables (Fig. S7; Table 2).

Growth environment influences on temperature response parameters

Variables describing the rate of a photosynthetic process were higher in sun compared to shade leaves, but

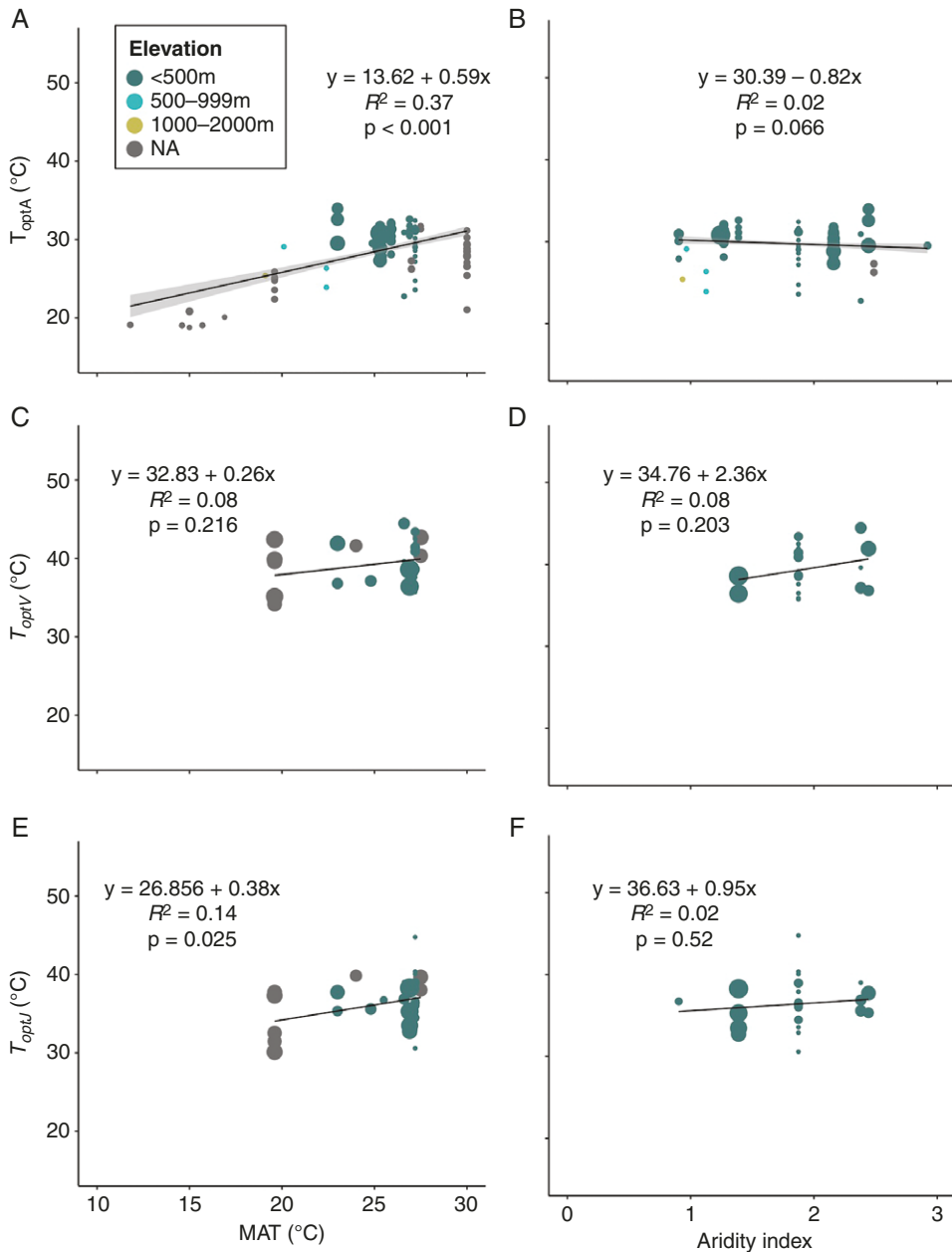


FIG. 1. The optimum temperature of net photosynthesis and biochemical responses to mean annual growth temperature and aridity index. T_{optA} response to (A) MAT and (B) aridity index. T_{optV} response to (C) MAT and (D) aridity index. T_{optJ} response to (E) MAT and (F) aridity index. Regression equations are weighted by number of observations that are used to calculate each temperature response mean. Size of data point depicts weight of each mean where larger data points carry a greater weight. Line represents linear regression fits (Table 2). Shaded area around line represents confidence intervals. Colour represents altitude groupings of <500 m (blue-green), 500–999 m (turquoise), 1000–2000 m (beige) and NA (grey). NA depicts data where elevation was not provided by the data author.

temperature response parameters did not differ. Sun and shade leaf T_{optA} were not significantly different from one another (Satterthwaite's method; $P = 0.786$; Fig. 4A). A_{25} of sun leaves was 1.5 times higher than that of shade leaves ($P = 0.008$; Fig. 4B). Similar to T_{optA} , there was no difference in Ω between the two light environments ($P = 0.210$; Fig. 4C). V_{25} and J_{25} of sun leaves were 88 % and 63 % higher than the rate of shade leaves, respectively (both $P < 0.001$; Fig. 4D, E), and $J:V$ was slightly (~10 %) higher in shade than in sun leaves ($P = 0.022$; Fig. 4F).

Plants grown *in situ* had higher biochemical response rates than *ex situ* grown plants, but this did not lead to differences in A_{sat} rates or parameters. There were no clear differences between plants grown *in* or *ex situ* for A_{sat} parameters and rates T_{optA} ($P = 0.085$), A_{25} ($P = 0.096$) or Ω ($P = 0.313$; Supplementary Data Fig. S8A–C). T_{optV} ($P = 0.974$; Fig. S7D) and E_{av} ($P = 0.102$; Fig. S8F) did not differ between *in* and *ex situ*, but plants grown *ex situ* had 40 % higher V_{25} ($P = 0.030$; Fig. S8E). T_{optJ} did not differ between growth environments ($P = 0.802$; Fig. S8G), J_{25} for plants grown *ex situ* was 48 %

TABLE 2. Regression equations for each photosynthetic parameter response to individual climate variables.

	Intercept	MAT slope	Coefficients		Marginal r^2	Conditional r^2	P-value
			Aridity index slope	T_{range} slope			
T_{opt}	13.62 ± 3.79	0.59 ± 0.15			0.37	0.78	<0.001
	30.39 ± 1.04		-0.82 ± 0.45		0.02	0.62	0.066
A_{25}	24.72 ± 2.45			0.25 ± 0.17	0.03	0.82	0.396
	1.67 ± 4.61	0.28 ± 0.19			0.05	0.27	0.139
Ω	8.35 ± 1.58		-0.46 ± 0.82		0.00	0.13	0.573
	9.38 ± 3.11			-8.02 × 10 ⁻² ± 24.24 × 10 ⁻²	0.00	0.26	0.741
T_{optV}	11.15 ± 7.77	0.14 ± 0.31			0.01	0.70	0.651
	15.35 ± 2.35		0.91 ± 0.82		0.01	0.80	0.268
V_{cmax}	11.30 ± 4.00			0.26 ± 0.29	0.01	0.69	0.380
	32.83 ± 5.26	0.26 ± 0.21			0.08	0.18	0.216
E_{av}	34.76 ± 3.68		2.36 ± 1.86		0.08	0.14	0.203
	35.91 ± 2.15			0.35 ± 0.24	0.10	0.25	0.156
V_{25}	75.26 ± 6.67	-1.36 ± 0.25			0.20	0.55	<0.001
	42.75 ± 3.78		-1.02 ± 1.33		0.01	0.26	0.443
E_{aj}	13.82 ± 6.76			2.16 ± 0.40	0.18	0.62	<0.001
	57.22 ± 89.50	1.54 ± 3.57			0.01	0.45	0.668
T_{optJ}	139.82 ± 69.15		-17.14 ± 33.39		0.02	0.44	0.608
	145.29 ± 45.95			-3.87 ± 3.47	0.09	0.45	0.264
J_{cmax}	26.56 ± 4.32	0.38 ± 0.17			0.14	0.14	0.025
	36.63 ± 2.86		0.95 ± 1.49		0.02	0.02	0.520
J_{max}	31.73 ± 3.33			0.35 ± 0.26	0.09	0.24	0.170
	182.95 ± 13.12	-4.37 ± 0.49			0.41	0.64	<0.001
$J:V$	76.39 ± 9.46		-0.91 ± 2.91		0.00	0.39	0.755
	-8.29 ± 14.68			6.43 ± 0.82	0.28	0.73	<0.001
$J:V$	-0.82 ± 91.11	3.08 ± 3.63			0.06	0.40	0.396
	108.84 ± 40.26		-11.00 ± 20.61		0.02	0.13	0.594
$J:V$	130.67 ± 48.49			-4.20 ± 3.64	0.08	0.41	0.249
	2.41 ± 0.16	-0.02 ± 0.01			0.10	0.53	<0.001
$J:V$	1.85 ± 0.14		7.64 × 10 ⁻³ ± 3.14 × 10 ⁻²		0.00	0.62	0.808
	1.50 ± 0.16			2.84 × 10⁻² ± 9.34 × 10⁻³	0.06	0.60	0.002

Photosynthetic parameters are: the optimum temperatures of net photosynthesis (T_{optA} ; °C), the rate of net photosynthesis at 25 °C (A_{25} ; $\mu\text{mol m}^{-2} \text{s}^{-1}$) at 25 °C, photosynthetic thermal niche or width of the temperature response curve (Ω ; °C), the optimum temperatures of the maximum rate of Rubisco carboxylation (V_{cmax}) and photosynthetic electron transport (J_{max}) (T_{optV} , T_{optJ} respectively; °C), the rate of V_{cmax} (V_{cmax} ; $\mu\text{mol m}^{-2} \text{s}^{-1}$) and J_{max} (J_{max} ; $\mu\text{mol m}^{-2} \text{s}^{-1}$) at 25 °C, and the activation energy term for V_{cmax} (E_{av} ; kJ mol^{-1}) and J_{max} (E_{aj} ; kJ mol^{-1}). Climate variables are mean annual temperature (MAT; °C), aridity index, and the mean annual temperature range from the maximum temperature of the warmest month and the minimum temperature of the coldest month. Intercepts and slopes are given as means ± s.e. Values in bold type indicate regression results with $P < 0.05$. Marginal r^2 provides the model variance of only the model fixed effect, whereas, conditional r^2 provides variance of the model with both the fixed and random effects.

higher than those grown *in situ* ($P = 0.054$; **Fig. S8H**) and E_{aj} was around double in *in situ* than in *ex situ* grown plants ($P = 0.002$; **Fig. S8I**). Lastly, $J:V$ also was not different between the two growth environments ($P = 0.696$; **Fig. S8J**).

Effects of plant functional type on temperature response parameters

T_{optA} was higher in drought (semi-) deciduous, or raingreen, species compared to broadleaf evergreen species, but other net

photosynthetic temperature response rates and variables did not differ between the two leaf habits. T_{optA} was ~1 °C higher in drought (semi-) deciduous compared with evergreen species ($P = 0.009$; **Fig. 5A**). There were no differences between evergreen and deciduous species for A_{25} ($P = 0.347$; **Fig. 5B**) or Ω ($P = 0.197$; **Fig. 5C**).

Optimum temperatures of photosynthesis did not vary between successional types, but rates of photosynthetic responses and the width of the photosynthetic responses were higher in early compared to mid/late successional species. Early and

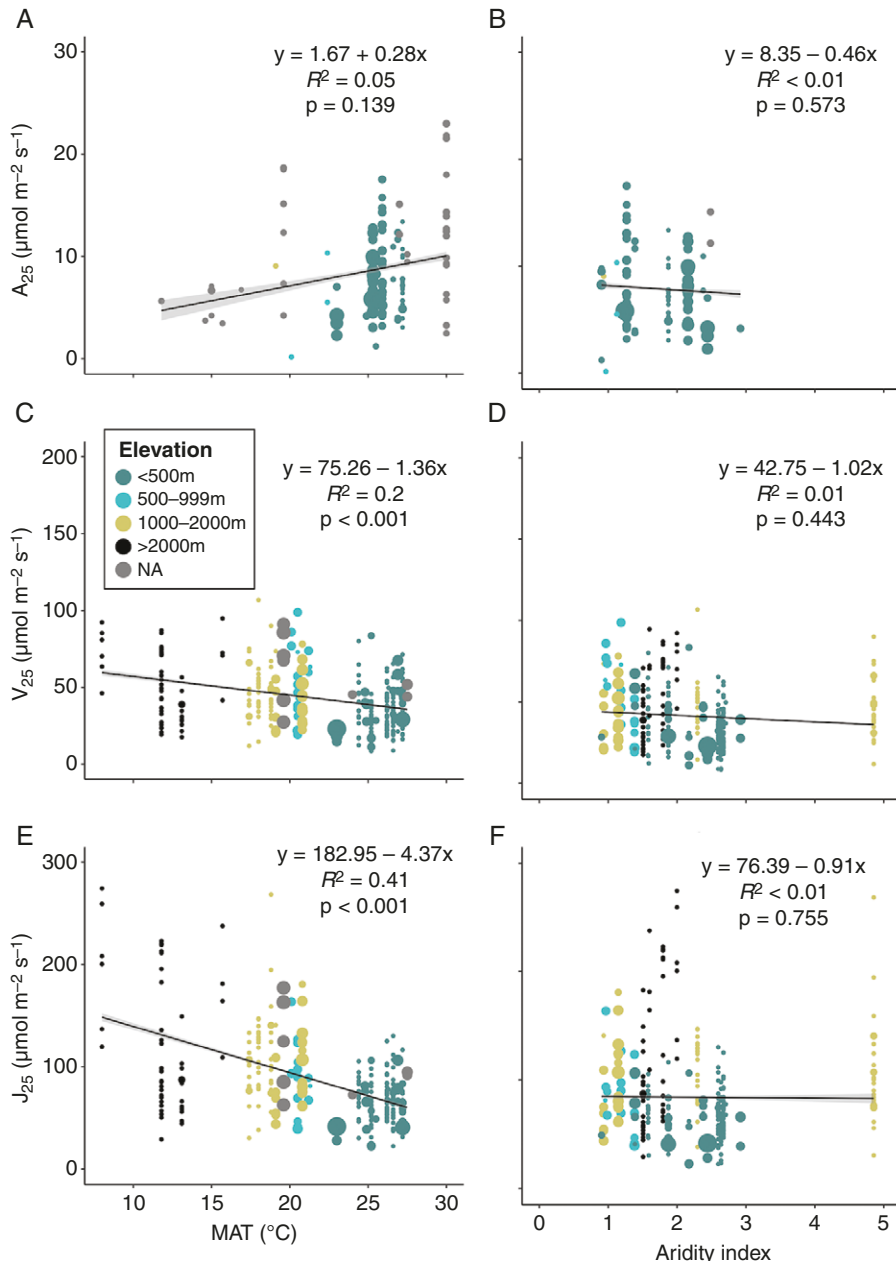


FIG. 2. The rate of net and the biochemical components of photosynthesis at 25 °C responses to three primary climate variables. A_{25} response to (A) MAT and (B) aridity index where higher aridity index indicates wetter conditions. V_{25} response to (C) MAT and (D) aridity index. J_{25} response to (E) MAT and (F) aridity index. Regression equations are weighted by number of observations used to calculate each temperature response mean. Size of data point depicts weight of each mean where larger data points carry a greater weight. Solid line represents significant linear regression fits (Table 2). Shaded area around line represents confidence intervals. Colour represents altitude groupings of <500 m (blue-green), 500–999 m (turquoise), 1000–2000 m (beige), >2000 m (black) and NA (grey). NA depicts data where elevation was not provided by the data author.

mid/late successional species did not differ in T_{optA} ($P = 0.955$; Fig. 6A). A_{25} and Ω (both $P < 0.001$; Fig. 6B, C) in early successional species were ~83 % and 32 % higher than in mid/late successional species, respectively. T_{optV} did not differ between successional types ($P = 0.502$; Fig. 6D) but, in terms of rates, mean early successional V_{25} was 61 % higher than late successional species ($P < 0.001$; Fig. 6E). There were no differences between successional types for $J:V$ ($P = 0.936$; Fig. 6F). T_{optJ} did not differ between successional types ($P = 0.644$; Fig. 6G)

but J_{25} for early successional species was around double that of late successional species ($P < 0.001$; Fig. 6H).

Hierarchical partitioning

Except for T_{optA} , hierarchical partitioning revealed that no single climate or growth environment variable explained a high amount of variation in our photosynthetic parameters. The strongest predictor for T_{optA} variation was elevation (individual

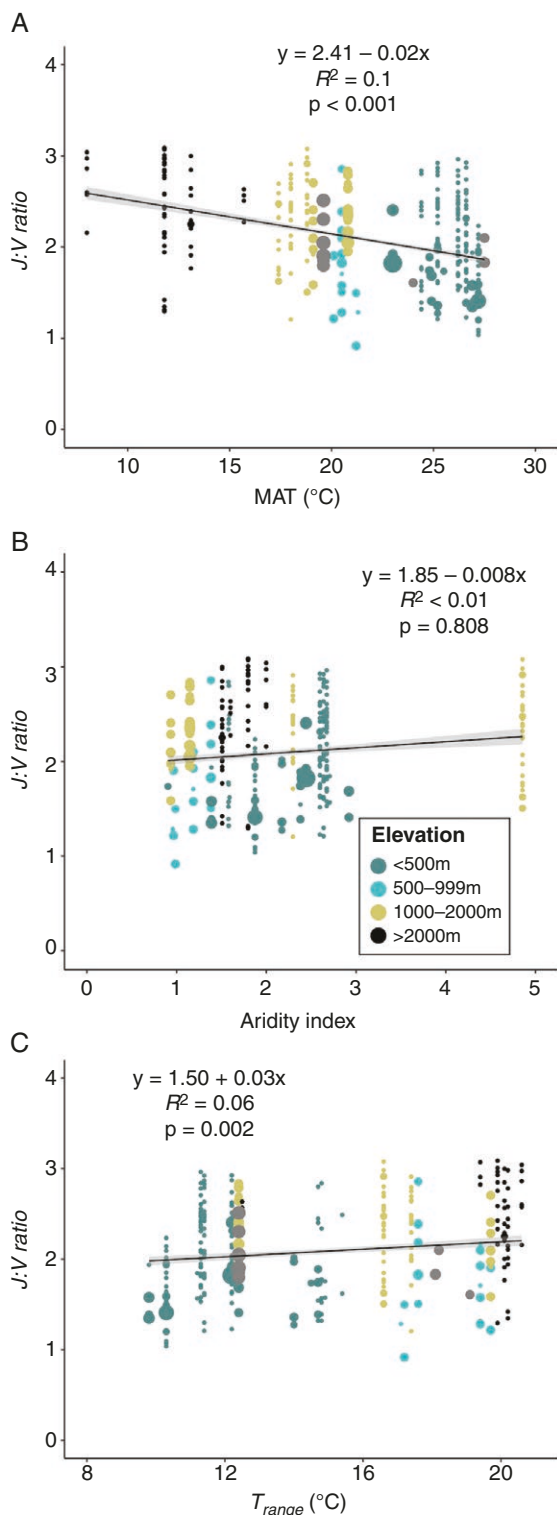


FIG. 3. The ratio between rate of J_{max} and V_{cmax} responses to three primary climate variables. The ratio between the rate of J_{max} at 25 °C and V_{cmax} at 25 °C (J:V) responses to (A) mean annual temperature (MAT), (B) aridity index and (C) mean annual temperature range (T_{range}). Regression equations are weighted by number of observations that are used to calculate each temperature response mean. Size of data point depicts the sample size used to weight each mean where larger data points carry a greater weight. Shaded area around line represents confident intervals. Colour represents altitude groupings of <500 m (blue-green), 500–999 m (turquoise), 1000–2000 m (beige), >2000 m (black) and NA (grey). NA depicts data where elevation was not provided by the data author.

adj $R^2 = 0.159$; Fig. 7A). With a full model $R^2 = 0.018$, climate was not a strong predictor for A_{25} ; however, MAT (adj $R^2 = 0.017$) had a slightly stronger individual effect on A_{25} than other predictors (Fig. 7B). Ω was more strongly predicted by T_{range} (adj $R^2 = 0.170$; Fig. 7C). T_{optV} was most strongly predicted by AI (adj $R^2 = 0.032$; Fig. 7D), V_{25} was slightly more predicted by MAT (adj $R^2 = 0.053$; Fig. 7E) and E_{av} was most strongly predicted by MAT (adj $R^2 = 0.128$; Fig. 7F). T_{optJ} was not well predicted by any climate variables; however, T_{range} explained slightly higher variation than other variables (adj $R^2 = -0.040$; Fig. 7G). Variance of J_{25} was more strongly explained by MAT (adj $R^2 = 0.125$; Fig. 6H). E_{av} was more strongly driven by MAT (adj $R^2 = 0.068$; Fig. 7I). J:V was best explained by elevation (adj $R^2 = 0.060$; Fig. 7J).

DISCUSSION

Climate drivers of the optimum temperature of photosynthesis

Globally (Kattge and Knorr, 2007; Kumarathunge *et al.*, 2019; Crous *et al.*, 2022) and in tropical ecosystems (Tan *et al.*, 2017), studies have found that the photosynthetic optimum temperature of net photosynthesis increases as growth temperatures increase. In partial support of our first hypothesis, the optimum temperatures of net photosynthesis (T_{optA}) and photosynthetic electron transport (T_{optJ}) rose with increasing MAT (Fig. 1A, E); however, the optimum temperature of Rubisco carboxylation (T_{optV}) did not (Fig. 1C). The slope of our tropical species responses to MAT (T_{optA} slope: 0.59 ± 0.15 °C °C⁻¹; Table 3) is similar to and has overlapping standard error with a global analysis of T_{optA} response to growth temperature (T_{optA} slope: 0.62 ± 0.1 °C per increase in growth temperature; Kumarathunge *et al.*, 2019), providing no evidence that different algorithms should be used to model tropical and global T_{optA} responses. T_{optJ} in our study also had a similar positive response as the global analysis (current study: T_{optJ} slope: 0.38 ± 0.17 MAT; Kumarathunge: T_{optJ} slope: $0.63 \pm 0.2 T_{\text{growth}}$; Kumarathunge *et al.*, 2019). Our results for the optimum temperatures of V_{cmax} were not as consistent with Kumarathunge *et al.* (2019), where our T_{optV} did not respond to MAT (T_{optV} slope: 0.26 ± 0.21 MAT; Table 3), but the global analysis showed a positive relationship with increasing growth temperature (T_{optV} slope: $0.71 \pm 0.2 T_{\text{growth}}$; Kumarathunge *et al.*, 2019). We note, however, that our meta-analysis of tropical species' biochemical parameters (19.6–27.5 °C) has a narrower temperature range than the global meta-analysis (~3.0–30.0 °C; Kumarathunge *et al.*, 2019) which, along with the high variation in parameter values at each point along the MAT axis, might limit our ability to detect data trends. Additionally, the lower T_{optV} MAT slope response provides some support for the common hypothesis that tropical species have adapted to narrower climate envelopes and do not respond strongly to variations in growth temperature, potentially resulting in a reduced capability to acclimate to higher temperatures (Janzen, 1967; Cunningham and Read, 2003; Dusenge *et al.*, 2021). This idea is further supported by Kumarathunge *et al.* (2019), who found optimum temperature responses to growth temperature were more strongly driven by acclimation to growth temperature than adaptation to climate of origin. In a recent analysis across latitudes, Crous *et al.* (2022) found more negative photosynthetic responses to higher temperatures in the tropics compared

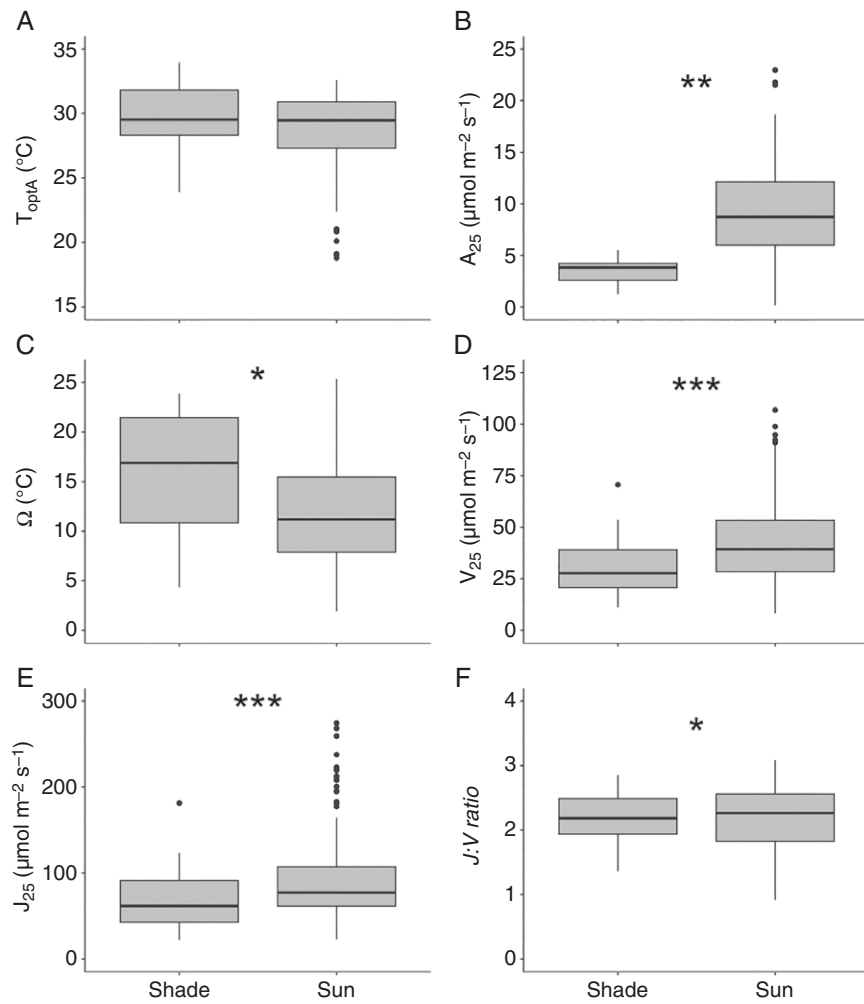


FIG. 4. Boxplots displaying the net photosynthetic and biochemistry at 25 °C parameter differences with leaf light environment. The distribution of shade and sun growth leaves for (A) T_{optA} , (B) A_{25} , (C) Ω , (D) V_{25} , (E) J_{25} and (F) the ratio of J_{max} to V_{max} . Ω indicates the difference in T_{opt} and the temperature where the rate of photosynthesis is 37 % of T_{opt} . The boxes display median and interquartile range. The whiskers represent 1.5 times the interquartile range. Data beyond the whiskers are outside of 1.5 times the interquartile range. Asterisks denote significant differences between treatments based on a Satterthwaite test: * $P < 0.05$, ** $P < 0.01$, *** $P < 0.001$. A_{max} : sun $n = 89$, shade $n = 6$; k_{25} : sun $n = 248$, shade $n = 23$.

to cooler climates, suggesting constrained acclimation. Our J_{max} and V_{max} temperature response datasets cover MAT across a reduced range (19.6–27.5 °C) than our A_{sat} dataset (11.8–30.0 °C). Additional studies investigating these biochemical parameters would enable the assessment of whether tropical forest species have systematically different temperature responses of these parameters than extra-tropical species.

Contrary to our hypothesis, AI alone was not a strong predictor of photosynthetic temperature responses. None of our photosynthetic parameters or rates responded to AI (Figs 1, 2, 3; Supplementary Data Fig. S7). Compared with trees in temperate zones, fewer studies in the tropics have investigated how rainfall affects T_{opt} . T_{optA} was found to increase as soils dry in a Puerto Rican tropical forest (Carter et al., 2020) and a savanna grassland ecosystem (Ma et al., 2017). However, Kumarathunge et al. (2020) found that the optimum temperature for tropical tree growth increases with water addition. Hierarchical partitioning showed AI as the most important measured climate component controlling T_{optV} ; however, the individual AI effect on T_{optV} was

very low (Fig. 7D). To date, the few studies that have investigated large-scale environmental controls on the biochemical components of photosynthesis have focused solely on how temperature controls these important model parameters (Kattge and Knorr, 2007; Tan et al., 2017; Kumarathunge et al., 2019; Crous et al., 2022). Even though these results suggest that aridity does not play a key role in controlling photosynthetic temperature responses, both temperature and rainfall play significant roles in modelled reductions in carbon gain in the Amazon rainforest (Galbraith et al., 2010). Future studies should investigate how other climate factors, such as aridity, influence photosynthetic optimum temperatures, as we know that a key constraint on photosynthetic optimization is the balance of carbon gain against water loss (Bloom et al., 1985; Wang et al., 2017).

Biochemical limitations at high temperatures

Limitations to the optimum temperature of net photosynthesis at moderate growth temperatures are often attributed

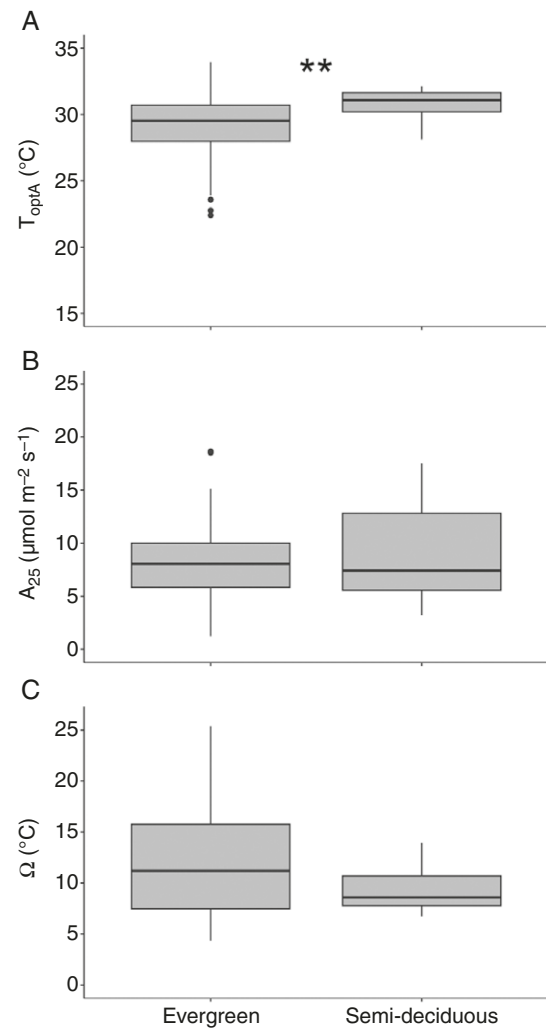


FIG. 5. Boxplots displaying the net photosynthetic parameter differences between species of different leaf habit. The distribution of evergreen and semi-deciduous species for (A) T_{optA} , (B) A_{25} and (C) Ω . The boxes display median and interquartile range. The whiskers represent 1.5 times the interquartile range. Data beyond the whiskers are outside of 1.5 times the interquartile range. Asterisks denote significant differences between treatments based on a Satterthwaite test: *** $P < 0.01$. Evergreen $n = 45$, semi-deciduous $n = 23$.

to limitations of Rubisco carboxylation temperature response parameters (Lin *et al.*, 2012; Yamaguchi *et al.*, 2016), although not always (Wise *et al.*, 2004; Cen and Sage, 2005). When plants are grown at elevated temperatures, measured photosynthesis is increasingly limited by carboxylation as temperature rises, a trend that is driven both by stomatal limitations on CO_2 substrate and by the high temperature sensitivity of Rubisco carboxylation (Brooks and Farquhar, 1985; Hikosaka *et al.*, 2006). However, optimality theory of photosynthetic capacity suggests that resources allocated to J_{\max} and V_{cmax} at 25 $^{\circ}\text{C}$ are disproportionately reduced under higher temperatures, resulting in reduced $J:\text{V}$ (Smith and Keenan, 2020; Wang *et al.*, 2020). The limitation to J_{\max} is due to high temperatures reducing electron transport through photosystem II (Havaux, 1996), and a greater investment in Rubisco carboxylation relative to electron transport to counteract the increased photorespiration at higher temperatures (Smith and Keenan, 2020).

This is supported by global meta-analyses showing declining $J:\text{V}$ with increasing growth temperature (Kumarathunge *et al.*, 2019; Crous *et al.*, 2022). Our results support this, where both V_{25} and J_{25} decreased with increasing MAT but J_{25} declined at a steeper rate (Fig. 2), resulting in a decreasing $J:\text{V}$ with rising MAT (Fig. 3). Across our temperature range, our results are not consistent with those of previous global meta-analyses (Medlyn *et al.*, 2002; Hikosaka *et al.*, 2006; Kattge and Knorr, 2007; Kumarathunge *et al.*, 2019), where neither of our activation energy terms of J_{\max} (E_{av}) or V_{cmax} (E_{av}) responded to temperature (Supplementary Data Fig. S8). E_{av} activation energy is a driver of V_{cmax} adjustment and is consistently found to increase with higher growth temperatures (Yamori *et al.*, 2005; Hikosaka *et al.*, 2006). The rate of E_{av} rise declines at temperatures that exceed mid 30 $^{\circ}\text{C}$, limiting V_{cmax} at higher temperatures (Scafaro *et al.*, 2023). The disparity between our results of no E_{av} response to growth temperature and $J:\text{V}$ results that are in line with global analyses could be due to the narrower temperature in our E_{av} dataset. Also, of note, this study does not consider effects of rising CO_2 concentrations on photosynthetic temperature responses. Elevated CO_2 can result in a positive shift in T_{opt} (Long, 1991; Šigut *et al.*, 2015), and this has been supported in studies on a subtropical tree species (Sheu and Lin, 1999) and a tropical mangrove species (Reef *et al.*, 2016). This response occurs because higher CO_2 concentrations can counteract the increased photorespiration rates that occur at higher temperatures, resulting in decreased $J:\text{V}$ (Long, 1991; Hikosaka *et al.*, 2006; but see Fauset *et al.*, 2019 in a tropical species). More CO_2 fertilization studies should be conducted in tropical forests to further elucidate interactions between tropical species CO_2 and temperature interaction responses.

Photosynthetic differences between growth conditions, deciduousness and successional types

We found that the rate of photosynthesis was higher in sun leaves but there were no T_{opt} differences between sun and shade leaves (Fig. 4), similar to the few studies that have investigated differences in *in situ* tropical photosynthetic responses to different canopy light conditions (Pearcy, 1987; Slot *et al.*, 2019; Hernández *et al.*, 2020; but see Carter *et al.*, 2021). Other biomes show similar results, and studies investigating differences in T_{optA} between upper canopy and understorey leaves have found that T_{optA} either does not differ (Carter and Cavaleri, 2018), or T_{optA} is higher in the upper canopy leaves (Jurik *et al.*, 1988). Niinemets *et al.* (1999) showed that the optimum temperature of electron transport is higher in the upper canopy (higher incident radiation on average) compared to lower canopy leaves (lower spectral quality, lower average incident radiation), suggesting that the biochemical process of photosynthesis associated with light can adjust to different light conditions and higher temperatures. Within the tropics, Carter *et al.* (2021) found that T_{optA} decreased as canopy height and light increased, probably due to vapour pressure deficit (VPD)-induced stomatal limitations. Hernández *et al.*, (2020) found trends toward higher T_{optV} in Panamanian sun leaves, yet T_{optV} did not differ between light conditions. We did not have enough V_{cmax} or J_{\max} data classified as 'shaded' and were unable to make a robust sun–shade comparison within our dataset. Even though

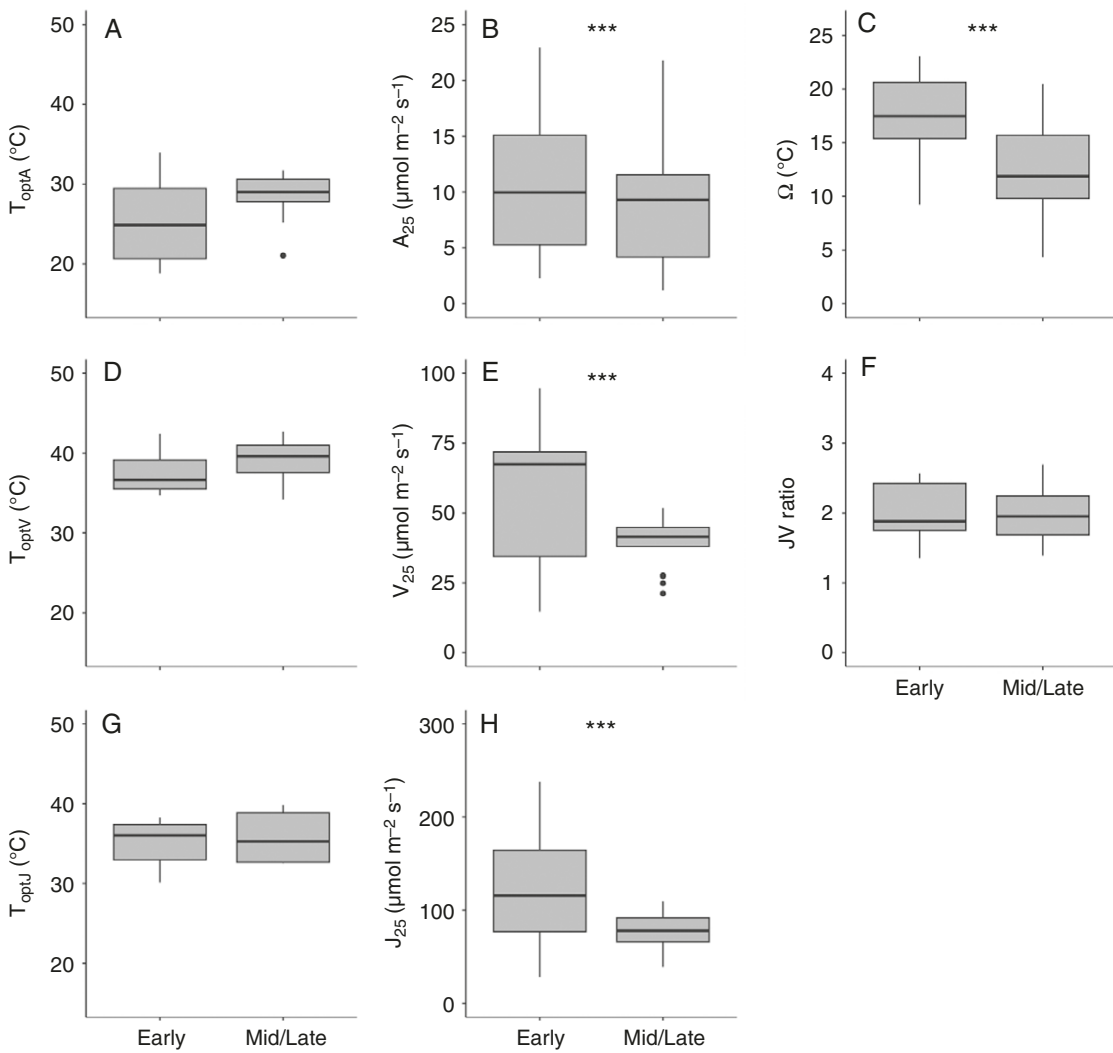


FIG. 6. Boxplots displaying the net photosynthetic parameter differences between successional strata. The distribution of early and late successional species for (A) T_{optA} , (B) A_{25} , (C) Ω , (D) T_{optV} , (E) V_{25} , (F) $J:V$, (G) T_{optL} and (H) J_{25} . The boxes display median and interquartile range. The whiskers represent 1.5 times the interquartile range. Data beyond the whiskers are outside of 1.5 times the interquartile range. Asterisks denote significant differences between treatments based on a Satterthwaite test: * $P < 0.05$, ** $P < 0.01$, *** $P < 0.001$. A_{max} : early $n = 20$, mid/late $n = 22$; k_{25} : early $n = 14$, shade $n = 17$; A–C: early $n = 8$, shade $n = 7$.

we were able to make a comparison between A_{sat} sun and shade leaves, we only had eight samples where shade leaves were measured (Supplementary Data Table S2), suggesting we need many more temperature response measurements comparing sun and shade leaves in tropical forests. Even so, the growing evidence in tropical forests suggests that light conditions do not strongly control tropical T_{opt} , and we may not need to distinguish between sun and shade leaves when modelling temperature responses in tropical forest canopies.

Even though leaf habits, such as evergreen and deciduous species, often have different photosynthetic temperature responses (Yamori *et al.*, 2014), global vegetation models usually do not implement separate temperature response parameters for different plant functional types due to insufficient data (Lombardozzi *et al.*, 2015; Smith *et al.*, 2016; Mercado *et al.*, 2018). In the current study, A_{25} did not differ but evergreen leaves had a slightly lower T_{optA} than semi-drought deciduous leaves (Fig. 5A, B). This suggests that global models should

differentiate between ‘broadleaf evergreen tropical’ and ‘semi-deciduous raingreen tropical’ forests (Poulter *et al.*, 2015), rather than considering all tropical regions as ‘broadleaf evergreen tropical’. Although we did find a trend toward higher T_{optA} in semi-deciduous species, we note that all species labelled as ‘semi-deciduous’ came from the same study (Slot and Winter, 2017a), which had the highest MAT (26.6 °C) of all the study sites included in the A_{sat} dataset. No species in our A – C dataset was characterized as either ‘deciduous’ or ‘semi-deciduous’ (Supplementary Data Table S1), preventing any analysis on differences between leaf habit for J_{max} and V_{cmax} data. Greater efforts should be made to better characterize differences between different plant functional types within the tropics and these data should be used to assess how vegetation models define tropical forest plant functional types.

Generally, fast growing, early successional species have higher rates of photosynthesis (Wright *et al.*, 2004). Our results agreed with this theory and, similar to Ziegler *et al.* (2020) and

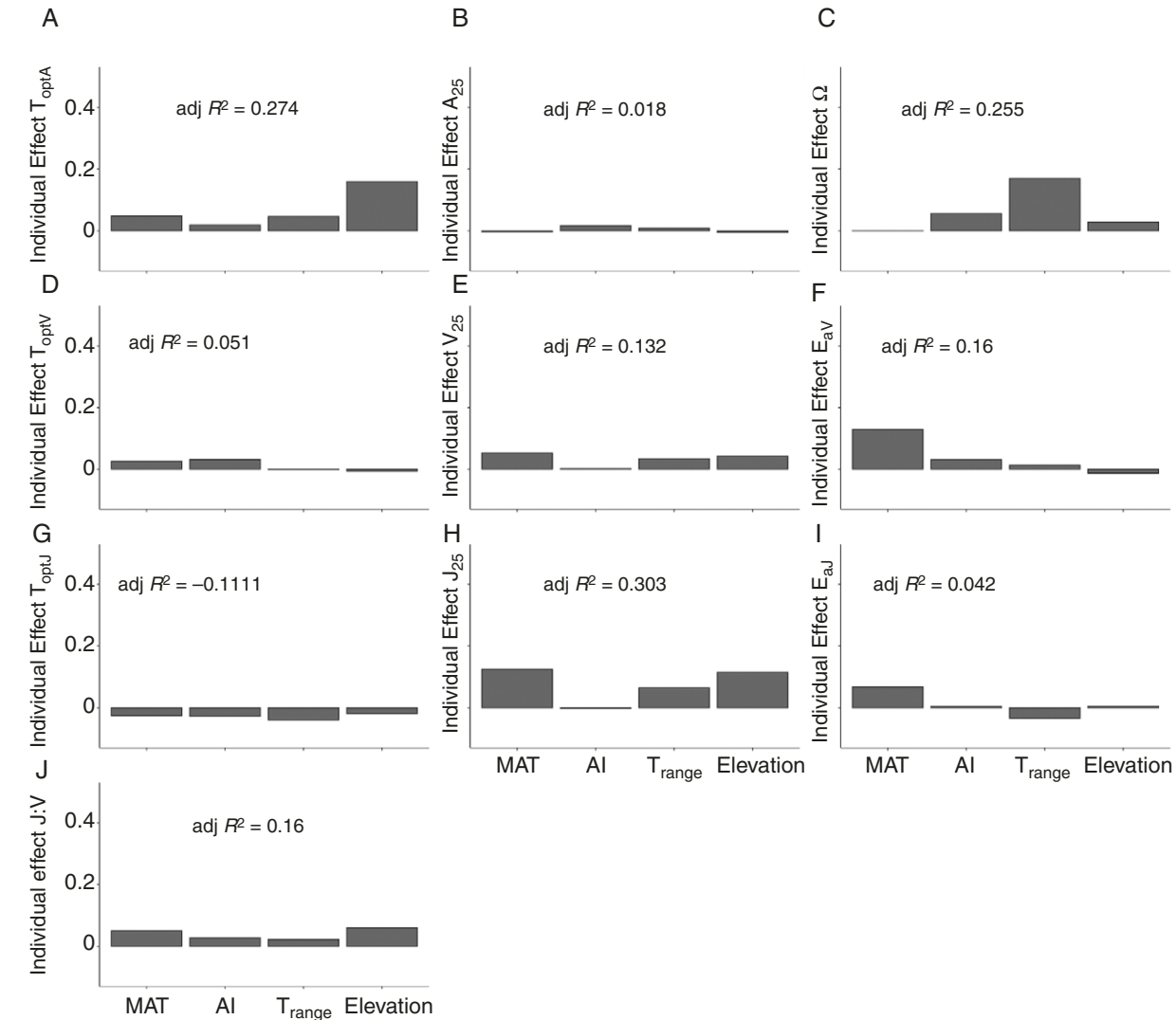


FIG. 7. Hierarchical partitioning results for relative individual importance of individual climate variables on T_{optA} (A), A_{25} (B), Ω (C), T_{optV} (D), V_{25} (E), H_{av} (F), H_{optU} (G), J_{25} (H), H_{ad} (I) and $J:V$ (J). Individual effect sums to the calculated total explained variation (adj R^2).

Mujawamariya *et al.* (2023), we found higher A_{25} , V_{25} and J_{25} in early successional species. Additionally, early successional species in a tropical dry forest were found to reside in higher temperature environments due to the higher light environment and more open forest structure in an early successional forest (Cao and Sanchez-Azofeifa, 2017), suggesting that early successional seedlings and saplings might have higher optimum temperatures. However, our study that combined all species growth stages found no differences between successional types for T_{optA} (Fig. 6). Our results support a lack of clear differences between canopy species of different successional types in Slot and Winter (2017b) but differ from the results of Slot *et al.* (2016), who found higher optimum temperatures in early successional seedlings. Here, we highlight that the study by Slot *et al.* (2016) was conducted on seedlings instead of canopy trees (Slot and Winter, 2017b). Future work should investigate differences in early successional seedling vs. mature canopy tree optimum temperatures. We did find that the net photosynthetic thermal niche (Ω) was broader for early successional species

than late successional species (Fig. 6C). This is consistent with theory on ‘fast’ species with high rates of photosynthesis, as these species tend to invest in traits that allow productivity under a wide range of temperatures (Michaletz *et al.*, 2016). A wider thermal niche is probably beneficial to early successional forests that experience a wider, more dynamic range of temperatures (Holbo and Luval, 1989).

Opportunities for better parameterized functions

We present trends for the temperature parameters of net photosynthetic and biochemical processes of net photosynthesis in tropical regions. However, both stomatal conductance and daytime respiration can also play large roles in controlling photosynthetic temperature responses (Lin *et al.*, 2012). Stomatal conductance or VPD, which is the primary climate variable controlling stomatal conductance (Farquhar and Sharkey, 1982), have been estimated to be the strongest predictors of photosynthetic decline with climate warming in the

tropics (Lloyd and Farquhar, 2008; Wu *et al.*, 2017; Smith *et al.*, 2020; Slot *et al.*, 2024). This relationship between temperature, moisture and stomatal conductance should also be investigated across tropical forests and is critical to understand photosynthetic responses to temperature as tropical forests become hotter and drier (Malhi *et al.*, 2008). Further, our hierarchical partitioning could be further improved if we had included leaf functional traits. Most of our photosynthetic parameters were not well explained by any environmental factors. A meta-analysis by Atkin *et al.* (2015) found that plant functional types (broadleaf, conifer, grass type, shrubs) had the most explanatory power for predicting the rate of respiration globally. In addition, other plant trait factors, such as leaf nitrogen and leaf mass per area, also improved their predictive models (Atkin *et al.*, 2015). Including other factors, such as leaf habit or growth type (e.g. evergreen or deciduous; successional type), could provide valuable information for tropical biome photosynthesis modelling, and substantial efforts should be made to collect a larger variation of these data types, which were not available for many of the studies we analysed. We also note that this study presents results that under-represent African and Asian tropical forests. Data from these regions could improve photosynthetic temperature response models.

CONCLUSIONS

This study reports new predictive equations that describe photosynthetic temperature responses of tropical trees to different climate factors and describes pan-tropic differences related to plant growth conditions, growth habits and successional strategies. Our novel analysis focusing on tropical woody species shows that T_{optA} and T_{optJ} responses to mean temperatures tended to align with global meta-analyses; however, the optimum temperature of T_{optV} did not align with results found globally. A lower slope of the photosynthetic biochemical parameter T_{opt} against MAT for tropical ecosystems suggests a lower capacity for these ecosystems to keep pace with climate change. While global carbon models should consider acclimation of the temperature response of photosynthetic parameters in order to allow for plant plasticity, the lower capacity for this response in tropical ecosystems should also be considered when making projections of ecosystem responses to climate change. Importantly, we did not find different temperature optima between sun/shade leaves or successional types, but we did find differences in optimum temperatures between evergreen and semi-deciduous species. Vegetation models often define these systems solely as ‘broadleaf evergreen tropical’, but functional types within tropical biomes have distinct temperature responses between ‘broadleaf evergreen tropical’ and ‘semi-deciduous rainforest tropical’ that should be considered to accurately represent tropical or global carbon dynamics.

SUPPLEMENTARY DATA

Supplementary data are available at *Annals of Botany* online and consist of the following.

Figure S1: PRISMA diagram outlining meta-analysis data selection and exclusion. Figure S2. Depiction of weighting factor ‘ J ’ at each mean annual temperature. Figure S3. Scatterplots of

the A_{sat} , $A-C_i$ and k_{25} dataset mean annual temperature (MAT) correlation with elevation. Figure S4. Boxplots displaying differences when photosynthetic biochemical parameters are estimated using temperature response variables estimated from global or only tropical studies. Figure S5. The optimum temperature of net photosynthesis and biochemical responses to mean annual temperature range of the average warmest day to the average coldest day. Figure S6. The rate of net photosynthesis and biochemical responses at 25 °C to mean annual temperature range of the average warmest day to the average coldest day. Figure S7. The net photosynthetic thermal niche and the activation energies of the biochemical components of photosynthesis responses to three primary climate variables. Figure S8. Boxplots displaying the differences in biochemical parameters of photosynthesis between plants grown *in* or *ex situ*. Table S1. List of A_{net} and J_{max}/V_{cmax} data sources. Table S2. Count of samples used in each type of light, leaf habit, successional status and growing environment. Table S3. Parameter estimates used to calculate V_{cmax} and J_{max} activation energies (E_{av} and E_{ar} , respectively), entropy terms (ΔS_v and ΔS_j , respectively), and deactivation terms (H_{dv} and H_{dr} , respectively) for this study (tropical) and a global analysis.

All data and analysis scripts can be found in Carter *et al.* 2025.

FUNDING

This work was supported by United States Geological Survey John Wesley Powell Center Working Center for Analysis and Synthesis. Funding was also provided by United States Department of Energy Office of Science, Biological and Environmental Research Program awards [DE-SC-0012000, DE-SC-0011806, DE-SC-0018942, 89243018S-SC-000014 and 89243018S-SC-000017]. Additional funding and support was provided by USDA Forest Service International Institute of Tropical Forestry (IITF). All research conducted at IITF is supported by the University of Puerto Rico. ORNL is managed by UT-Battelle, LLC, for the Department of Energy under contract DE-AC05-1008 00OR22725. APW, SPS, AR and KSE. were supported by the Next Generation Ecosystem Experiments-Tropics (NGEE Tropics), funded by the United States Department of Energy, Office of Science, Office of Biological and Environmental Research, AR, KSE and SPS were also partially supported by the United States Department of Energy contract No. DE-SC0012704 to Brookhaven National Laboratory, and AR and KSE by the United States Department of Energy Contract No. DE-AC02-05CH11231 to Lawrence Berkeley National Laboratory. KYC gratefully acknowledges the Australian Research Council [DE160101484] supporting data collection on some Australian species. The contribution of PBR was supported by a United States National Science Foundation Biological Integration Institutes grant [DBI-2021898]. Any use of trade, firm or product names is for descriptive purposes only and does not imply endorsement by the United States Government. JW acknowledges the funding support from the National Natural Science Foundation of China [#31922090] and the Innovation and Technology Fund (funding support to State Key Laboratories in Hong Kong of Agrobiotechnology) of the HKSAR, China.

ACKNOWLEDGEMENTS

Author contributions: KRC, MAC, AR, SPS, KSE, RJN, APW, PBR, SCR, TEW conceived of and designed the study, KRC and ECS organized and analysed the data. KRC and MAC wrote the manuscript. KRC, AR, KSE, OA, NHAB, AWC, ZC, KYC, CED, MED, JRE, JFS, JWGK, ACM, BEM, PM, JR, MS, EST, JU, AV, KW, JW collected and contributed data to the study. All authors contributed to writing and editing the final manuscript.

DATA AVAILABILITY

All data and analysis scripts can be found in [Carter et al., 2025](#).

LITERATURE CITED

Anderegg WRL, Schwalm C, Biondi F, et al. 2015. Pervasive drought legacies in forest ecosystems and their implications for carbon cycle models. *Science* **349**: 528–532.

Arneth A, Mercado L, Kattge J, Booth BBB. 2012. Future challenges of representing land-processes in studies on land-atmosphere interactions. *Biogeosciences* **9**: 3587–3599.

Atkin OK, Bloomfield KJ, Reich PB, et al. 2015. Global variability in leaf respiration in relation to climate, plant functional types and leaf traits. *The New Phytologist* **206**: 614–636.

Bates D, Meachler M, Bolker B, S W. 2015. Fitting linear mixed-effects models using lme4. *Journal of Statistical Software* **67**: 1–48.

Battaglia M, Beadle C, Loughhead S. 1996. Photosynthetic temperature responses of *Eucalyptus globus* and *Eucalyptus nitens*. *Tree Physiology* **16**: 81–89.

Berry J, Björkman O. 1980. Photosynthetic response and adaptation to temperature in higher plants. *Annual Review of Plant Physiology* **31**: 491–543.

Bloom AJ, Chapin FS, Mooney HA. 1985. Plants—an economic analogy. *Annual Review of Ecological Systems* **16**: 363–392.

Booth BBB, Jones CD, Collins M, et al. 2012. High sensitivity of future global warming to land carbon cycle processes. *Environmental Research Letters* **7**: 024002.

Box E. 1996. Plant functional types and climate at the global scale. *Journal of Vegetation Science* **7**: 309–320.

Brooks A, Farquhar GD. 1985. Effect of temperature on the CO_2/O_2 specificity of ribulose-1,5-bisphosphate carboxylase/oxygenase and the rate of respiration in the light - Estimates from gas-exchange measurements on spinach. *Planta* **165**: 397–406.

Cao S, Sanchez-Azofeifa A. 2017. Modeling seasonal surface temperature variations in secondary tropical dry forests. *International Journal of Applied Earth Observation and Geoinformation* **62**: 122–134.

Carswell FE, Costa AL, Palheta M, et al. 2002. Seasonality in CO_2 and H_2O flux at an eastern Amazonian rain forest. *Journal of Geophysical Research: Atmospheres* **107**: LBA 43-1–LBA 43-16.

Carter KR, Cavalieri MA. 2018. Within-canopy experimental leaf warming induces photosynthetic decline instead of acclimation in two Northern hardwood Species. *Frontiers in Forests and Global Change* **1**: 20181219. doi:10.3389/ffgc.2018.00011

Carter K, Cavalieri M, Atkin O, et al. 2025. Tropical Photosynthetic Temperature Response Meta-Analysis datasets: Effects of Hurricane Disturbance and Increased Temperature on Carbon Cycling and Storage of a Puerto Rican Forest: A Mechanistic Investigation of Above- and Belowground Processes. *Dataset*. doi:10.15485/2513897

Carter KR, Wood TE, Reed SC, et al. 2020. Photosynthetic and respiratory acclimation of understory shrubs in response to in situ experimental warming of a wet tropical forest. *Frontiers in Forests and Global Change* **3**: 1–20.

Carter KR, Wood TE, Reed SC, Butts KM, Cavalieri MA. 2021. Experimental warming across a tropical forest canopy height gradient reveals minimal photosynthetic and respiratory acclimation. *Plant Cell and Environment* **44**: 2879–2897.

Cavalieri MA, Reed SC, Smith WK, Wood TE. 2015. Urgent need for warming experiments in tropical forests. *Global Change Biology* **21**: 2111–2121.

Cavalieri MA, Coble AP, Ryan MG, Bauerle WL, Loescher HW, Oberbauer SF. 2017. Tropical rainforest carbon sink declines during El Niño as a result of reduced photosynthesis and increased respiration rates. *New Phytologist* **216**: 136–149.

Cen YP, Sage RF. 2005. The regulation of Rubisco activity in response to variation in temperature and atmospheric CO_2 partial pressure in sweet potato. *Plant Physiology* **139**: 979–990.

Choury Z, Wujeska-Klause A, Bourne A, et al. 2022. Tropical rainforest species have larger increases in temperature optima with warming than warm-temperate rainforest trees. *The New Phytologist* **234**: 1220–1236.

Cox AJF, Hartley IP, Meir P, et al. 2023. Acclimation of photosynthetic capacity and foliar respiration in Andean tree species to temperature change. *The New Phytologist* **238**: 2329–2344.

Crous KY, Uddling J, De Kauwe MG. 2022. Temperature responses of photosynthesis and respiration in evergreen trees from boreal to tropical latitudes. *The New Phytologist* **234**: 353–374.

Crous KY, Cheesman AW, Middleby K, et al. 2023. Similar patterns of leaf temperatures and thermal acclimation to warming in temperate and tropical tree canopies. *Tree Physiology* **43**: 1383–1399.

Cunningham S, Read J. 2002. Comparison of temperate and tropical rainforest tree species: photosynthetic responses to growth temperature. *Oecologia* **133**: 112–119.

Cunningham SC, Read J. 2003. Do temperate rainforest trees have a greater ability to acclimate to changing temperatures than tropical rainforest trees? *The New Phytologist* **157**: 55–64.

Curtis PS, Wang X. 1998. International association for ecology a meta-analysis of elevated CO_2 effects on woody plant mass, form, and physiology. *Oecologia* **113**: 299–313.

De Pury DGG, Farquhar GD. 1997. Simple scaling of photosynthesis from leaves to canopies without the errors of big-leaf models. *Plant, Cell and Environment* **20**: 537–557.

Diffenbaugh NS, Scherer M. 2011. Observational and model evidence of global emergence of permanent, unprecedented heat in the 20th and 21st centuries. *Climatic Change* **107**: 615–624.

Dixon RK, Brown S, Houghton RA, Solomon AM, Trexler MC, Wisniewski J. 1994. Carbon pools and flux of global forest ecosystems. *Science* **263**: 185–190.

Doughty CE, Goulden ML. 2008. Are tropical forests near a high temperature threshold? *Journal of Geophysical Research* **113**: G00–B07.

Doughty CE, Keany JM, Wiebe BC, et al. 2023. Tropical forests are approaching critical temperature thresholds. *Nature* **621**: 105–111.

Dusenge ME, Duarte AG, Way DA. 2019. Plant carbon metabolism and climate change: elevated CO_2 and temperature impacts on photosynthesis, photorespiration and respiration. *The New Phytologist* **221**: 32–49.

Dusenge ME, Wittmann M, Mujawamariya M, et al. 2021. Limited thermal acclimation of photosynthesis in tropical montane tree species. *Global Change Biology* **27**: 4860–4878.

Duursma RA. 2015. Plantecophys - an R package for analysing and modelling leaf gas exchange data. *PLoS One* **10**: e0143346.

Farquhar GD, Sharkey TD. 1982. Stomatal conductance and photosynthesis. *Annual Review of Plant Physiology* **33**: 317–345.

Farquhar GD, Caemmerer SV, Berry J. 1980. A biochemical model of photosynthesis CO_2 fixation in leaves of C3 species. *Planta* **149**: 78–90.

Faust S, Freitas HC, Galbraith DR, et al. 2018. Differences in leaf thermoregulation and water-use strategies between three co-occurring Atlantic forest tree species. *Plant, Cell & Environment* **41**: 1618–1631.

Faust S, Oliveira L, Buckeridge MS, et al. 2019. Contrasting responses of stomatal conductance and photosynthetic capacity to warming and elevated CO_2 in the tropical tree species *Alchornea glandulosa* under heatwave conditions. *Environmental and Experimental Botany* **158**: 28–39.

Fick SE, Hijmans RJ. 2017. WorldClim 2: new 1-km spatial resolution climate surfaces for global land areas. *International Journal of Climatology* **37**: 4302–4315.

Fisher RA, Koven CD, Anderegg WRL, et al. 2018. Vegetation demographics in earth system models: a review of progress and priorities. *Global Change Biology* **24**: 35–54.

Friedlingstein P, Cox P, Betts R, et al. 2006. Climate-carbon cycle feedback analysis: results from the C4MIP model intercomparison. *Journal of Climate* **19**: 3337–3353.

Galbraith D, Levy PE, Sitch S, et al. 2010. Multiple mechanisms of Amazonian forest biomass losses in three dynamic global vegetation models under climate change. *The New Phytologist* **187**: 647–665.

Goulden ML, Miller SD, Da Rocha HR, et al. 2004. Diel and seasonal patterns of tropical forest CO₂ exchange. *Ecological Applications* **14**: 42–54.

Green JK, Berry J, Ciais P, Zhang Y, Gentile P. 2020. Amazon rainforest photosynthesis increases in response to atmospheric dryness. *Science Advances* **6**: 1–10.

Greve P, Seneviratne SI. 2015. Assessment of future changes in water availability and aridity. *Geophysical Research Letters* **42**: 5493–5499.

Guan K, Pan M, Li H, et al. 2015. Photosynthetic seasonality of global tropical forests constrained by hydroclimate. *Nature Geoscience* **8**: 284–289.

Gurevitch J, Morrow LL, Wallace A, Walsh JS. 1992. A meta-analysis of competition in field experiments. *The American Naturalist* **140**: 539–572.

Havaux M. 1996. Short-term response of photosystem I to heat stress. *Photosynthesis Research* **47**: 85–97.

Hedges LV, Olkin I. 1985. *Statistical methods for meta-analysis*. New York: Academic Press.

Hernández GG, Winter K, Slot M. 2020. Similar temperature dependence of photosynthetic parameters in sun and shade leaves of three tropical tree species. *Tree Physiology* **40**: 637–651.

Hikosaka K, Ishikawa K, Borjigidai A, Muller O, Onoda Y. 2006. Temperature acclimation of photosynthesis: Mechanisms involved in the changes in temperature dependence of photosynthetic rate. *Journal of Experimental Botany* **57**: 291–302.

Holbo HR, Luval JC. 1989. Modeling surface temperature distributions in forest landscapes. *Remote Sensing of Environment* **27**: 11–24.

Janzen DH. 1967. Why mountain passes are higher in the tropics. *The American Naturalist* **101**: 233–249.

Jaramillo C, Ochoa D, Contreras L, et al. 2010. Effects of rapid global warming at the Paleocene–Eocene boundary on neotropical vegetation. *Science* **330**: 957–961.

June T, Evans JR, Farquhar GD. 2004. A simple new equation for the reversible temperature dependence of photosynthetic electron transport: a study on soybean leaf. *Functional Plant Biology* **31**: 275–283.

Jurik TW, Weber JA, Gates DM. 1988. Effects of temperature and light on photosynthesis of dominant species of a northern hardwood forest. *Botanical Gazette* **149**: 203–208.

Kattge J, Knorr W. 2007. Temperature acclimation in a biochemical model of photosynthesis: a reanalysis of data from 36 species. *Plant, Cell and Environment* **30**: 1176–1190.

Kattge J, Knorr W, Raddatz T, Wirth C. 2009. Quantifying photosynthetic capacity and its relationship to leaf nitrogen content for global-scale terrestrial biosphere models. *Global Change Biology* **15**: 976–991.

Kitajima K, Mulkey SS, Wright SJ. 1997. Seasonal leaf phenotypes in the canopy of a tropical dry forest: photosynthetic characteristics and associated traits. *Oecologia* **109**: 490–498.

Kotsup B, Montped P, Kasemsap P, Thaler P, Améglio T, Dreyer E. 2009. Photosynthetic capacity and temperature responses of photosynthesis of rubber trees (*Hevea brasiliensis* Müll. Arg.) acclimate to changes in ambient temperatures. *Trees - Structure and Function* **23**: 357–365.

Kullberg AT, Slot M, Feeley KJ. 2023. Thermal optimum of photosynthesis is controlled by stomatal conductance and does not acclimate across an urban thermal gradient in six subtropical tree species. *Plant Cell and Environment* **46**: 831–849.

Kumarathunge DP, Medlyn BE, Drake JE, et al. 2019. Acclimation and adaptation components of the temperature dependence of plant photosynthesis at the global scale. *The New Phytologist* **222**: 768–784.

Kumarathunge DP, Drake JE, Tjoelker MG, et al. 2020. The temperature optima for tree seedling photosynthesis and growth depend on water inputs. *Global Change Biology* **26**: 2544–2560.

Lai J, Zou Y, Zhang J, Peres-Neto PR. 2022. Generalizing hierarchical and variation partitioning in multiple regression and canonical analyses using the rdacca.R package. *Methods in Ecology and Evolution* **13**: 782–788.

Lin YS, Medlyn BE, Ellsworth DS. 2012. Temperature responses of leaf net photosynthesis: the role of component processes. *Tree Physiology* **32**: 219–231.

Lloyd J, Farquhar GD. 2008. Effects of rising temperatures and [CO₂] on the physiology of tropical forest trees. *Philosophical Transactions of the Royal Society of London, Series B: Biological Sciences* **363**: 1811–1817.

Lombardozzi DL, Bonan GB, Smith NG, Dukes JS, Fisher RA. 2015. Temperature acclimation of photosynthesis and respiration: a key uncertainty in the carbon cycle-climate feedback. *Geophysical Research Letters* **42**: 8624–8631.

Long SP. 1991. Modification of the response of photosynthetic productivity to rising temperature by atmospheric CO₂ concentrations: has its importance been underestimated? *Plant, Cell & Environment* **14**: 729–739.

Ma S, Osuna JL, Verfaillie J, Baldocchi DD. 2017. Photosynthetic responses to temperature across leaf–canopy–ecosystem scales: a 15-year study in a Californian oak–grass savanna. *Photosynthesis Research* **132**: 277–291.

Malhi Y, Roberts JT, Betts R, Killeen TJ, Li W, Nobre C. 2008. Climate change, deforestation, and the fate of the Amazon. *Science* **319**: 169–172.

Marshall B, Biscoe PV. 1980. A model for C3 leaves describing the dependence of net photosynthesis on irradiance II. *Journal of Experimental Botany* **31**: 41–48.

Matthews HD, Eby M, Ewen T, Friedlingstein P, Hawkins BJ. 2007. What determines the magnitude of carbon cycle-climate feedbacks? *Global Biogeochemical Cycles* **21**: 1–12.

Mau A, Reed S, Wood T, Cavalieri M. 2018. Temperate and tropical forest canopies are already functioning beyond their thermal thresholds for photosynthesis. *Forests* **9**: 47.

Medlyn BE, Dreyer E, Ellsworth D, et al. 2002. Temperature response of parameters of a biochemically based model of photosynthesis. II. A review of experimental data. *Plant, Cell and Environment* **25**: 1167–1179.

Mercado LM, Medlyn BE, Huntingford C, et al. 2018. Large sensitivity in land carbon storage due to geographical and temporal variation in the thermal response of photosynthetic capacity. *The New Phytologist* **218**: 1462–1477.

Michaletz ST, Weiser MD, McDowell NG, et al. 2016. The energetic and carbon economic origins of leaf thermoregulation. *Nature Plants* **2**: 1–8.

Miller BD, Carter KR, Reed SC, Wood TE, Cavalieri MA. 2021. Only sun-lit leaves of the uppermost canopy exceed both air temperature and photosynthetic optima in a wet tropical forest. *Agricultural and Forest Meteorology* **301–302**: 108347.

Mora C, Frazier AG, Longman RJ, et al. 2013. The projected timing of climate departure from recent variability. *Nature* **502**: 183–187.

Mujawamariya M, Wittemann M, Dusenge ME, et al. 2023. Contrasting warming responses of photosynthesis in early- and late-successional tropical trees. *Tree Physiology* **43**: 1104–1117.

Niinemets U. 2007. Photosynthesis and resource distribution through plant canopies. *Plant, Cell and Environment* **30**: 1052–1071.

Niinemets U, Oja V, Kull O. 1999. Shape of leaf photosynthetic electron transport versus temperature response curve is not constant along canopy light gradients in temperate deciduous trees. *Plant, Cell & Environment* **22**: 1497–1513.

Oliver RJ, Mercado LM, Clark DB, et al. 2022. Improved representation of plant physiology in the JULES-vn.5 land surface model: photosynthesis, stomatal conductance and thermal acclimation. *Geoscientific Model Development* **15**: 5567–5592.

Pan Y, Birdsey RA, Phillips OL, Jackson RB. 2013. The structure, distribution, and biomass of the world's forests. *Annual Review of Ecology, Evolution, and Systematics* **44**: 593–622.

Pearcy R. 1987. Photosynthetic gas exchange responses of Australian tropical forest trees in canopy, gap and understorey micro-environments. *Functional Ecology* **1**: 169–178.

Poulter B, MacBean N, Hartley A, et al. 2015. Plant functional type classification for Earth system models: results from the European Space Agency's land cover climate change initiative. *Geoscientific Model Development* **8**: 2315–2328.

R Core Team. 2020. *R: A Language and Environment for Statistical Computing*. Vienna: R Foundation for Statistical Computing.

Read J. 1990. Some effects of acclimation temperature on net photosynthesis in some tropical and extra-tropical Australasian Nothofagus species. *Journal of Ecology* **78**: 100–112.

Reef R, Slot M, Motro U, et al. 2016. The effects of CO₂ and nutrient fertilisation on the growth and temperature response of the mangrove *Avicennia germinans*. *Photosynthesis Research* **129**: 159–170.

Reich PB, Bermudez R, Montgomery RA, et al. 2022. Even modest climate change may lead to major transitions in boreal forests. *Nature* **608**: 540–545.

Rey-Sánchez A, Slot M, Posada J, Kitajima K. 2016. Spatial and seasonal variation in leaf temperature within the canopy of a tropical forest. *Climate Research* **71**: 75–89.

Rogers A, Medlyn BE, Dukes JS, et al. 2017. A roadmap for improving the representation of photosynthesis in Earth system models. *The New Phytologist* **213**: 22–42.

Ryu Y, Baldochei DD, Kobayashi H, et al. 2011. Integration of MODIS land and atmosphere products with a coupled-process model to estimate gross primary productivity and evapotranspiration from 1 km to global scales. *Global Biogeochemical Cycles* **25**.

Santos A, Carvalho W, Morel J, et al. 2018. Variations in precipitation and the equilibrium dynamics of a tropical forest tree community in south-eastern Brazil. *Journal of Tropical Forest Science* **30**: 597–605.

Scafaro AP, Xiang S, Long BM, et al. 2017. Strong thermal acclimation of photosynthesis in tropical and temperate wet-forest tree species: the importance of altered Rubisco content. *Global Change Biology* **23**: 2783–2800.

Scafaro AP, Posch BC, Evans JR, Farquhar GD, Atkin OK. 2023. Rubisco deactivation and chloroplast electron transport rates co limit photosynthesis above optimal leaf temperature in terrestrial plants. *Nature Communications* **14**: 1–9.

Sheu BH, Lin CK. 1999. Photosynthetic response of seedlings of the subtropical tree *Schima superba* with exposure to elevated carbon dioxide and temperature. *Environmental and Experimental Botany* **41**: 57–65.

Šigut L, Holíšová P, Klem K, et al. 2015. Does long-term cultivation of saplings under elevated CO₂ concentration influence their photosynthetic response to temperature? *Annals of Botany* **116**: 929–939.

Sinclair TR, Murphy CE, Knoerr KR. 1976. Development and evaluation of simplified models for simulating canopy photosynthesis and transpiration. *Journal of Applied Ecology* **13**: 813–829.

Slot M, Winter K. 2017a. In situ temperature response of photosynthesis of 42 tree and liana species in the canopy of two Panamanian lowland tropical forests with contrasting rainfall regimes. *New Phytologist* **214**: 1103–1117.

Slot M, Winter K. 2017b. Photosynthetic acclimation to warming in tropical forest tree seedlings. *Journal of Experimental Botany* **68**: 2275–2284.

Slot M, Winter K. 2018. High tolerance of tropical sapling growth and gas exchange to moderate warming. *Functional Ecology* **32**: 599–611.

Slot M, Rey-Sánchez C, Gerber S, Lichstein JW, Winter K, Kitajima K. 2014. Thermal acclimation of leaf respiration of tropical trees and lianas: response to experimental canopy warming, and consequences for tropical forest carbon balance. *Global Change Biology* **20**: 2915–2926.

Slot M, Garcia MA, Winter K. 2016. Temperature response of CO₂ exchange in three tropical tree species. *Functional Plant Biology* **43**: 468–478.

Slot M, Krause GH, Krause B, Hernández GG, Winter K. 2019. Photosynthetic heat tolerance of shade and sun leaves of three tropical tree species. *Photosynthesis Research* **141**: 119–130.

Slot M, Rifai SW, Eze CE, Winter K. 2024. The stomatal response to vapor pressure deficit drives the apparent temperature response of photosynthesis in tropical forests. *New Phytologist* **244**: 1238–1249.

Smith NG, Dukes JS. 2013. Plant respiration and photosynthesis in global-scale models: Incorporating acclimation to temperature and CO₂. *Global Change Biology* **19**: 45–63.

Smith NG, Keenan TF. 2020. Mechanisms underlying leaf photosynthetic acclimation to warming and elevated CO₂ as inferred from least-cost optimality theory. *Global Change Biology* **26**: 5202–5216.

Smith NG, Malyshev SL, Sheviakova E, Kattge J, Dukes JS. 2016. Foliar temperature acclimation reduces simulated carbon sensitivity to climate. *Nature Climate Change* **6**: 407–411.

Smith MN, Taylor TC, van Haren J, et al. 2020. Empirical evidence for resilience of tropical forest photosynthesis in a warmer world. *Nature Plants* **6**: 1225–1230.

Tagesson T, Schurgers G, Horion S, et al. 2020. Recent divergence in the contributions of tropical and boreal forests to the terrestrial carbon sink. *Nature Ecology and Evolution* **4**: 202–209.

Tan ZH, Zeng J, Zhang YJ, et al. 2017. Optimum air temperature for tropical forest photosynthesis: Mechanisms involved and implications for climate warming. *Environmental Research Letters* **12**: 054022.

Van Schaik E, Killaars L, Smith NE, et al. 2018. Changes in surface hydrology, soil moisture and gross primary production in the Amazon during the 2015/2016 El Niño. *Philosophical Transactions of the Royal Society B: Biological Sciences* **373**: 20180084.

Vargas GG, Cordero SRA. 2013. Photosynthetic responses to temperature of two tropical rainforest tree species from Costa Rica. *Trees* **27**: 1261–1270.

Värhammar A, Wallin G, McLean CM, et al. 2015. Photosynthetic temperature responses of tree species in Rwanda: evidence of pronounced negative effects of high temperature in montane rainforest climax species. *The New Phytologist* **206**: 1000–1012.

von Caemmerer S, Farquhar GD. 1981. Some relationships between the biochemistry of photosynthesis and the gas exchange of leaves. *Planta* **153**: 376–387.

Wang YP, Leuning R. 1998. A two-leaf model for canopy conductance, photosynthesis and partitioning of available energy I: model description and comparison with a multi-layered model. *Agricultural and Forest Meteorology* **91**: 89–111.

Wang H, Prentice IC, Davis TW, Keenan TF, Wright IJ, Peng C. 2017. Photosynthetic responses to altitude: an explanation based on optimality principles. *The New Phytologist* **213**: 976–982.

Wang H, Atkin OK, Keenan TF, et al. 2020. Acclimation of leaf respiration consistent with optimal photosynthetic capacity. *Global Change Biology* **26**: 2573–2583.

Way DA, Oren R. 2010. Differential responses to changes in growth temperature between trees from different functional groups and biomes: a review and synthesis of data. *Tree Physiology* **30**: 669–688.

Way DA, Yamori W. 2014. Thermal acclimation of photosynthesis: On the importance of adjusting our definitions and accounting for thermal acclimation of respiration. *Photosynthesis Research* **119**: 89–100.

Williams JW, Jackson ST, Kutzbach JE. 2007. Projected distributions of novel and disappearing climates by 2100 AD. *Proceedings of the National Academy of Sciences of the United States of America* **104**: 5738–5742.

Wise RR, Olson AJ, Schrader SM, Sharkey TD. 2004. Electron transport is the functional limitation of photosynthesis in field-grown *Pima* cotton plants at high temperature. *Plant, Cell and Environment* **27**: 717–724.

Wittemann M, Andersson MX, Nitrugulirwa B, Tarvainen L, Wallin G, Uddling J. 2022. Temperature acclimation of net photosynthesis and its underlying component processes in four tropical tree species. *Tree Physiology* **42**: 1188–1202.

Wright IJ, Westoby M, Reich PB, et al. 2004. The worldwide leaf economics spectrum. *Nature* **428**: 821–827.

Wu J, Albert LP, Lopes AP, et al. 2016. Leaf development and demography explain photosynthetic seasonality in Amazon evergreen forests. *Science* **351**: 972–976.

Wu J, Guan K, Hayek M, et al. 2017. Partitioning controls on Amazon forest photosynthesis between environmental and biotic factors at hourly to interannual timescales. *Global Change Biology* **23**: 1240–1257.

Yamaguchi DP, Nakaji T, Hiura T, Hikosaka K. 2016. Effects of seasonal change and experimental warming on the temperature dependence of photosynthesis in the canopy leaves of *Quercus serrata*. *Tree Physiology* **36**: 1283–1295.

Yamori W, Noguchi K, Terashima I. 2005. Temperature acclimation of photosynthesis in spinach leaves: analyses of photosynthetic components and temperature dependencies of photosynthetic partial reactions. *Plant, Cell & Environment* **28**: 536–547.

Yamori W, Hikosaka K, Way DA. 2014. Temperature response of photosynthesis in C3, C4, and CAM plants: Temperature acclimation and temperature adaptation. *Photosynthesis Research* **119**: 101–117.

Yan J, Zhang Y, Yu G, et al. 2013. Seasonal and inter-annual variations in net ecosystem exchange of two old-growth forests in southern China. *Agricultural and Forest Meteorology* **182–183**: 257–265.

Zarakas CM, Swann ALS, Koven C, Marielle N, Taylor TC. 2024. Different model assumptions about plant hydraulics and photosynthetic temperature acclimation yield diverging implications for tropical forest resilience. *Global Change Biology* **30**: 1–16.

Ziegler C, Dusenge ME, Nyirambangutse B, Zibera E, Wallin G, Uddling J. 2020. Contrasting dependencies of photosynthetic capacity on leaf nitrogen in early- and late-successional tropical montane tree species. *Frontiers in Plant Science* **11**: 1–12.